Recent changes of relative humidity: regional connection with land and ocean processes

Sergio M. Vicente-Serrano[1], Raquel Nieto[2], Luis Gimeno[2], Cesar Azorin-Molina[3], Anita Drumond[2], Ahmed El Kenawy[1,4], Fernando Dominguez-Castro[1], Miquel Tomas-Burguera[5], Marina Peña-Gallardo[1]

[1] Instituto Pirenaico de Ecología, Consejo Superior de Investigaciones Científicas (IPE–CSIC), Zaragoza, Spain; [2]Environmental Physics Laboratory, Universidade de Vigo, Ourense, Spain. [3]Regional Climate Group, Department of Earth Sciences, University of Gothenburg, Sweden. [4]Department of Geography, Mansoura University, Mansoura, Egypt; [5]Estación Experimental Aula Dei, Consejo Superior de Investigaciones Científicas (EEAD-CSIC), Zaragoza, Spain;

* Corresponding author: svicen@ipe.csic.es

Abstract. We analyzed changes in surface relative humidity (RH) at the global scale from 1979 to 2014 using both observations and ERA-Interim dataset. We compared the variability and trends of RH with those of land evapotranspiration and ocean evaporation in moisture source areas across a range of selected regions worldwide. The sources of moisture for each particular region were identified by integrating different observational data and model outputs into a lagrangian approach. The aim was to account for the possible role of changes in air temperature over land, in comparison to sea surface temperature (SST), but also the role of land evapotranspiration and the ocean evaporation on RH variability. Results suggest an agreement between the interannual variability of RH and the interannual variability of precipitation and land evapotranspiration in regions with continentally-originated humidity. In contrast, albeit with the dominant positive trend of air temperature/SST ratio in the majority of the analyzed regions, the interannual variability of RH in the target regions did not show any significant correlation with this ratio over the source regions. Also, we did not find any significant association between the interannual variability of oceanic evaporation in the oceanic humidity source regions and RH in the target regions. Our findings stress the need for further investigation of the role of both dynamic and radiative factors in the evolution of RH over continental regions at different spatial scales.

Key-words: Relative humidity; Evaporation; Evapotranspiration; Moisture; Trends; Oceans.

1. Introduction

Relative Humidity (RH) is a key meteorological parameter that determines the aerodynamic component of the atmospheric evaporative demand (AED) (Wang and Dickinson, 2012; McVicar et al., 2012a). As such, changes in RH may impact significantly the evolution of the AED (Vicente-Serrano et al., 2014a), with particular implications for the intensity of the hydrological cycle (Sherwood, 2010), climate aridity (Sherwood and Fu, 2014) as well as severity of drought events (Rebetez et al., 2006; Marengo et al., 2008).

In a changing climate, temperature rise, as suggested by different climate scenarios, may impact the atmospheric humidity. According to the Classius-Clapeyron (CC) relationship, a temperature rise of 1 ºC is sufficient to increase the equilibrium amount of water vapor of the air by roughly 7%. Given the unlimited water availability in the oceans as well as the projected temperature rise, water vapor content is expected to increase, at least in the oceanic areas, in order to maintain RH constant in future. Particularly, there is empirical evidence on the increase in the water vapor content at both the surface and upper tropospheric levels (Trenberth et al., 2005). In this context, numerous studies have supported the constant RH scenario under global warming conditions (e.g. Dai, 2006; Lorenz and Deweaver 2007; Willett et al., 2008; McCarthy et al., 2009; Ferraro et al., 2015). In contrast, other studies supported the non-stationary behavior of RH, not only in continental areas located far from oceanic humidity (e.g. Pierce et al., 2013), but also in humid regions (e.g. Van Wijngaarden and Vincent, 2004). Assuming the stationary behavior of RH, the influence of RH on AED may be constrained, given that any possible change in AED would be mostly determined by changes in other aerodynamic variables (e.g. air temperature and wind speed) (McVicar et al., 2012a and b) or by changes in cloudiness and solar radiation (Roderick and Farquhar, 2002; Fan and Thomas, 2013). However, a range of studies have supported the non-stationary behavior of RH under global warming, giving insights on significant changes in RH over the past decades. A representative example is Simmons et al. (2010) who compared gridded observational and reanalysis RH data, suggesting a clear dominant negative trend in RH over the Northern Hemisphere since 2000. Also, based on a newly developed homogeneous gridded database that employed the most available stations from the telecommunication system of the WMO, Willett et al. (2014) found significant negative changes in RH, with strong spatial variability, at the global scale. This global pattern was also confirmed at the regional scale, but with different signs of change, including both negative (e.g. Vincent et al., 2007; Vicente-Serrano e al., 2014b; 2016; Zongxing et al., 2014) and positive trends (e.g. Shenbin, 2006; Jhajharia et al., 2009; Hosseinzadeh Talaee et al., 2012).

There are different hypotheses that explain the non-stationary evolution of RH under global warming conditions. One of these hypotheses is related to the slower warming of oceans in comparison to continental areas (Lambert and Chiang, 2007; Joshi et al., 2008). In particular, specific humidity of air advected from oceans to continents increases more slowly than saturation specific humidity over land (Rowell and Jones 2006; Fasullo 2010). This would decrease RH over continental areas, inducing an increase in AED and aridity conditions (Sherwood and Fu, 2014). Some studies employed global climate models (GCMs) to support this hypothesis under future warming conditions (e.g. Joshi et al., 2008; O’Gorman and Muller, 2010; Byrne and O’Gorman, 2013). However, empirical studies that support this hypothesis using observational data are unavailable. Moreover, the observed decrease in RH over some coastal areas, which are adjacent to their sources of moisture, adds further uncertainty to this hypothesis (Vicente-Serrano et al., 2014b and 2016; Willet et al., 2014).

Another hypothesis to explain the non-stationary evolution of RH is associated with land-atmosphere feedback processes. Different studies indicated that atmospheric moisture and precipitation are strongly linked to moisture recycling in different regions of the world (e.g. Rodell et al., 2015). Thus, evapotranspiration may contribute largely to water vapor content and precipitation over land (Stohl and James, 2005; Bosilovich and Chern, 2006; Trenberth et al., 2007; Dirmeyer et al., 2009; van der Ent et al., 2010). Land-atmospheric feedbacks may also have marked influence on atmospheric humidity (Seneviratne et al., 2006); given that soil drying can suppress evapotranspiration, reduce RH and thus reinforce AED. All these processes would again reinforce soil drying (Seneviratne et al., 2002; Berg et al., 2016).

Indeed, it is very difficult to determine which hypothesis can provide an understanding of the observed RH trends at the global scale. Probably, the two hypotheses combined together can be responsible for the observed RH trends in some regions of the world (Rowell and Jones, 2006). In addition to the aforementioned hypotheses, some dynamic forces, which are associated with atmospheric circulation processes, can explain the non-stationary behavior or RH worldwide (e.g., Goessling and Reick, 2011). However, defining the relative importance of these physical processes in different world regions is quite challenging (Zhang et al., 2013; Laua and Kim, 2015).

The objective of this study is to compare the recent variability and trends of RH with changes in the two types of fluxes that affect RH: i) vertical fluxes that were assessed using land evapotranspiration and precipitation and ii) advection that was quantified using oceanic evaporation from moisture source areas. The novelty of this work stems from the notion that although different studies have already employed GCM’s and different scenarios to explain the possible mechanisms behind RH changes under warming conditions, we introduce a new empirical approach that employs different observational data sets, reanalysis fields and a lagrangian-based approach, not only for identifying the continental and oceanic moisture areas for different target regions, but also for exploring the relevance of the existing hypothesis to assess the magnitude, sign and spatial patterns of RH trends in the past decades at the global scale.

2. Data and methods

2.1. Data

2.1.1. Observation RH data set

We employed the monthly RH HadISDH dataset, available through http://www.metoffice.gov.uk/hadobs/hadisdh/. This dataset represents the most complete and accurate global dataset for RH, including observational data from a wide range of stations worldwide (Willet et al., 2014). Given that HadISDH includes some series with data gaps; our decision was to choose only those series with no more than 20% of missing values over the period 1979-2014. In order to fill these gaps, we created a standardized regional series for each station using the most correlated series with each target series. While this procedure maintains the temporal variance of the original data, it provides a low biased estimation of the missing values. In order to avoid biases in the filling due to differences in the distribution parameters (mean and variance) between the candidate and the objective data series, a bias correction was performed on the candidate data. Thus, normal distribution was used for bias correction of RH. The data of the candidate series were re-scaled to match the statistical distribution of the observed series to be filled, based on the overlapping period between them. Overall, a final dataset of 3462 complete stations spanning different regions worldwide and covering the period 1979-2014 was employed in this work.

2.1.2. Reanalysis RH dataset

Daily data of dewpoint (T_d), air temperature (T) and surface pressure (P_{mst}) at a spatial interval of 0.5° was obtained from the ERA-Interim covering the period 1979-2014 (http://www.ecmwf.int/en/research/climate-reanalysis/era-interim) (Dee et al., 2011). To calculate RH we followed the formulation used by Willett et al. (2014) for the HadISDH RH dataset. The reason for this is to make better comparable the RH obtained from observations in the HadISDH and the RH obtained from the ERA-Interim dataset. Based on the selected variables, we calculated the daily RH following Buck (1981):

$$RH = 100\left(\frac{e}{e_s}\right) \qquad (1)$$

where *e* is the actual vapor pressure in hPa and e_s is the saturated vapor pressure in hPa. As a function of the wet bulb air temperature (T_w) in ºC, *e* is estimated following two different equations with respect to water/ice. If T_w is above 0ºC, *e* is calculated as :

$$e = 6.1121 \cdot f_w exp\left(\frac{\left(18.729-\left[\frac{T_d}{227.3}\right]\right)\cdot T_d}{257.78+T_d}\right) \qquad (2)$$

Where T_d is the dew point temperature in ºC

If T_w is below 0ºC, *e* it is calculated as:

$$e = 6.1115 \cdot f_i exp\left(\frac{\left(23.036-\left[\frac{T_d}{333.7}\right]\right)\cdot T_d}{279.82+T_d}\right) \qquad (3)$$

where

$$f_w = 1 + 7 \times 10^{-4} + 3.46 \times 10^{-6} P_{mst} \qquad (4)$$

$$f_i = 1 + 3 \times 10^{-4} + 4.18 \times 10^{-6} P_{mst} \qquad (5)$$

Where P_{mst} is the pressure at the height level.

T_w is obtained according to Jensen et al. (1990):

$$T_w = \frac{aT + bT_d}{a+b} \qquad (6)$$, where

$$a = 6.6 \times 10^{-5} P_{mst} \qquad (7)$$

$$b = \frac{409.8e}{(T_d+237.3)^2} \qquad (8)$$

and T is the 2 meters air temperature in ºC

e_s is obtained by substituting T_d by T .

2.1.3. Land precipitation and land air temperature

We employed the gridded land precipitation and surface air temperature data (TS v.3.23), provided by the Climate Research Unit (UK), at a 0.5º spatial interval for the period 1979-2014 (Harris et al., 2014). This product was developed using a relatively high number of observational sites, which guarantees a robust representation of climatic conditions across worldwide regions. Importantly, this product has been carefully tested for potential data inhomogenities as well as anomalous data.

2.1.4. Sea Surface Temperature (SST)

We used the monthly SST data (HadSST3), compiled by the Hadley Centre for the common period 1979-2014 (http://www.metoffice.gov.uk/hadobs/hadsst3/). This dataset is provided at a 0.5º grid interval (Kennedy et al., 2011a and b).

2.1.5. Ocean evaporation and continental evapotranspiration data

To quantify the temporal variability and trends of land evapotranspiration and oceanic evaporation, we employed two different datasets. First, the oceanic evaporation was quantified using the Objectively Analyzed air-sea Fluxes (OAFLUX) product (Yu et al., 2008) from 1979 to 2014, which was used to analyze recent variability and changes in evaporation from global oceans (Yu, 2007). To account for land evapotranspiration, we employed the Global Land Evaporation Amsterdam Model (GLEAM) (Version 3.0a) (http://www.gleam.eu/) (Miralles et al., 2011) from 1980 to 2014. This data set has been widely validated using in situ measurements of surface soil moisture and evaporation across the globe (Martens et al., 2016).

2.2. Methods

2.2.1. Relative Humidity (RH) trends

We assessed the seasonal (boreal cold season: October-March; boreal warm season: April-September) and annual trends of RH for 1979-2014 using two different global datasets (HadISDH and ERA-Interim). To quantify the magnitude of change in RH, we used a linear regression analysis between the series of time (independent variable) and RH series (dependent variable). The slope of the regression indicates the amount of change (per year), with higher slope values indicating greater changes. To assess the statistical significance of the detectable changes, we applied the nonparametric Mann–Kendall statistic, which measures the degree to which a trend is consistently increasing or decreasing (Zhang et al., 2001). To account for any possible influence of serial autocorrelation on the robustness of the defined trends, we applied the modified Mann–Kendall trend test, which returns the corrected p-values after accounting for temporal pseudoreplication in RH series (Hamed and Rao, 1998; Yue and Wang, 2004). The statistical significance of the trend was tested at the 95% confidence level ($p<0.05$).

Following the trend analysis results, we selected those regions that showed a high agreement between HadISDH and ERA-Interim datasets in terms of the sign and magnitude of RH changes. Nevertheless, we also extended our selection to some other regions, with low station density in the HadISDH dataset. This decision was simply motivated by the consistent changes found over these regions, as suggested by the ERA-Interim dataset. For all the defined regions, we identified the oceanic and continental moisture sources by means of the FLEXPART lagrangian model.

2.2.2. Identification of continental and oceanic moisture sources

We used the FLEXPART V9.0 particle dispersion model fed with the ERA-Interim reanalysis data. According to this model, the atmosphere is divided homogeneously into three-dimensional finite elements (hereafter “particles”); each represents a fraction of the total atmospheric mass (Stohl and James, 2004). These particles may be advected backward or forward in time using three-dimensional wind taken from the ERA-Interim data every time step, with superimposed stochastic turbulent and convective motions. The rates of increase (e) and decrease (p) of moisture (e-p) along the trajectory of each particle were calculated via changes in the specific moisture (q) with time (e-p = mdq/dt), where m is the mass of the particle. Similar to the wind field, q is also taken from the meteorological data. FLEXPART allows identifying the particles affecting a particular region using information about the trajectories of these selected particles. A description of this methodology is detailed in Stohl and James (2004).

The FLEXPART dataset used in this study was provided by a global experiment in which the entire global atmosphere was divided into approximately 2.0 million “particles”. The tracks were computed using the ERA-Interim reanalysis data at 6 h intervals, at a 1º horizontal resolution and at a vertical resolution of 60 levels from 0.1 to 1000 hPa. For each particular target region, all the particles were tracked backward in time, and its position and specific humidity (q) were recorded every 6 h. With this methodology, the evaporative sources and sink regions for the particles reaching the target region can be identified. All areas where the particles gained humidity ($E - P > 0$) along their trajectories towards the target region can be considered as “sources of moisture”. In contrast, all areas with lost humidity ($E - P < 0$) are considered as “sinks”.

A typical period used to track the particles backward in time is 10 days that is the average residence time of water vapor in the global atmosphere (Numaguti, 1999). However, we followed the methodology of Miralles et al (2016), where an optimal lifetime of vapor in the atmosphere was calculated to reproduce the sources of moisture. As such, three steps were carried out in this order: i) all the particles that leave each target region were tracked back during 15 days and the "initial sources" at annual scale were defined as those areas with positive (E-P) values, ii) from these "initial sources", all the particles were forward tracked during 1 to 15 days individually, and (E-P)<0 was calculated for these lifetime periods to estimate the precipitation contribution over the target region, iii) the optimal lifetime selected for each region was chosen according to the minimum absolute difference between the FLEXPART simulated precipitation and the CRU TS v.3.23 for each region, iv) and finally the backward tracking was recalculated during these optimal lifetimes.

We defined the climatological spatial extent of each source region corresponding to a particular target region by applying a 95th percentile criterion computed for the annual and seasonal (boreal summer and winter) positive (E-P) field (Vazquez et al., 2016). Then, for each year of the period, we estimated the total moisture supply from each source region.

Also from FLEXPART simulations, we obtained the fractions of moisture from the continental and oceanic sources annually and for each cold and warm season. The purpose was to compare with the results obtained on the role of the land evapotranspiration and ocean evaporation of RH variability and trends.

2.2.3. Relationship between RH and the selected land/oceanic climate variables

Based on defining the spatial extent of each moisture source region, we calculated annual, warm and cold season regional series for ocean evaporation and land evapotranspiration using the OAFLUX and GLEAM datasets, respectively. The regional series of ocean evaporation and land evapotranspiration were created using a weighted average based on the seasonal/annual fields of (E-P)>0 (Section 2.2.2). This approach allows creating a time series that better represents the interannual variability of ocean evaporation and land evapotranspiration in the source(s) of moisture for each defined region. Following the same approach, we also calculated the regional series of SST corresponding to each oceanic moisture source region. Likewise, we calculated the regional series of land precipitation and air temperature for each target region using CRU TS v.3.23 dataset, and the ratio between air temperature in the target region and SST in the source region.

For each target region, we related the regional series of seasonal and annual RH with the corresponding regional times series of all aforementioned climatic variables. However, to limit the possible influence of the trends presented in the data itself on the computed correlations, we de-trended the series of the climate variables prior to calculating the correlation. We also assessed changes in the regional series of the different variables; their statistical significance was tested by means of the modified Mann-Kendall test at the 95% level. For each target region, we summarized the results of the magnitude of change in RH as well as other investigated variables at the seasonal and annual scales. However, to facilitate the comparison among the different variables and the target regions worldwide, we transformed the amount of change of each variable to percentages.

Finally, we also computed the association between RH and land evapotranspiration at the annual and seasonal scales using the available gridded evapotranspiration series. While a pixel-to-pixel comparison does not produce a reliable assessment of the possible contribution of land evapotranspiration to RH changes, given that the source of moisture can apparently be far from the target region, we still believe that this association can give insights on the possible relationship between land evapotranspiration on RH changes.

3. Results

3.1. Trends in Relative Humidity

Supplementary Figure 1 shows the average seasonal and annual RH and the Vertically Integrated Moisture Flux (VIMF), which can be used to estimate regions where the precipitation dominates (negative values) over the evaporation (positive values), from the ERA-Interim dataset. RH shows higher average values over equatorial regions, Southeast Asia and the North Eurasia region. The lower values are recorded over tropical regions, mainly in the North Hemisphere. Spatial differences between the cold and warm regions are very low. The annual pattern of the VIFM over continents shows that precipitation exceeds evaporation over the Intertropical Convergence Zone, Southeast Asia and the islands between Pacific and Indian Oceans (Maritime continent), a great part of South America, Central America, Central Africa, and northward to 40ºN in the Northern Hemisphere. Evaporation is higher than precipitation over the main area of Australia, the Pacific coast of North America, Northeast Brazil, areas around Mediterranean Sea, Eastern coast of Africa and southwest Asia. Seasonally it is evident the poleward movement of the ITCZ during the hemispheric summer, and the change of the pattern over North America and Eurasian continent.

Figure 1 summarizes the magnitude of change in RH for the boreal cold and warm seasons and at the annual scale, calculated using the annual and seasonal (boreal summer and winter) for the period between 1979 and 2014. For HadISDH, it is noted that the available RH stations is unevenly distributed over the globe, with higher density in the mid-latitudes of the Northern Hemisphere. Nevertheless, the available stations show coherent and homogeneous spatial patterns of RH changes. In the boreal cold season, the most marked decrease was observed in the Southwest and areas of Northeast North America, central Argentina, the Fertile Crescent region in western Asia, Kazakhstan, as well as in the eastern China and the Korea Peninsula. On the other hand, dominant RH increase was recorded in larger areas, including most of Canada (mostly in the Labrador Peninsula), and large areas of North and central Europe and India. While the density of complete and homogeneous RH series is low, we found a dominant positive trend across the western Sahel and South Africa. The ERA-Interim dataset showed magnitudes of change close to those suggested by HadISDH. In addition, the ERA-Interim also provides information on RH changes in regions with low density of RH observations (e.g. East Amazonian, east Sahel and Iran), suggesting a dominant RH decrease across these regions.

For the boreal warm season, a clear tendency towards a reduction in RH was observed in vast regions of the world, including (mostly the Iberian Peninsula, France, Italy, Turkey and Morroco), Eastern Europe, and western part of Russia. Based on the available stations across central Asia, we also found a general reduction of RH; a similar pattern was also observed in East Asia, including Mongolia, east China, north Indonesia, south Japan and Korea. This reduction was also noted South America, with a general homogeneous pattern over Peru, Bolivia and a strong decrease over central Argentina. On the other hand, the positive evolution of RH observed during the cold season across Canada and Scandinavia was reinforced during the boreal warm season. In the west Sahel and India, we found an upward trend of RH. The ERA-Interim also revealed a strong RH decrease over the whole Amazonian region and the West Sahel, while a marked increase dominated over the Andean region between Colombia, Ecuador and North Peru. In Australia, the spatial patterns were more complex than those obtained using the available observatories.

The HadISDH dataset suggests a general decrease of RH over Southwest North America, Argentina, central Asia, Turkey, Mongolia and China, with a particular reduction over the East Sahel, Iran, Mongolia and the eastern Asia. On the other hand, a dominant positive trend was observed across Canada, areas of North Southern America, the western Sahel, South Africa (Namibia and Botswana), some areas of Kenia, India and the majority of Australia. A wide range of these regions exhibited statistically significant trends from 1979 to 2014. (Supplementary Figure 2). A statistically significant negative trend was observed at the seasonal and annual scales, not only in most of Southern America and Northern America, but in large regions of Africa, South Europe, central and East Asia as well. On the other hand, areas of complex topography in the Northern Hemisphere, Australia, India, Northern South America and Africa showed positive trends.

Albeit with these complex spatial patterns of RH changes, there is a globally dominant negative trend (Figure 2). This pattern was observed using both the HadISDH and the ERA-Interim datasets, although there is marked spatial bias in data availability of the HadISDH. Figure 3 illustrates the relationship between the magnitudes of change in RH, as suggested by the HadISDH dataset versus the ERA-Interim dataset. At the seasonal and annual scales, there is a relatively high correlation (mostly above 0.55). Given this high consistency between the HadISDH and the ERA-Interim datasets in terms of both the magnitude and sign of change in RH (Figures 1 and 2) and also in interannual variations (Supplementary Figures 3 and 4), we decided to restrict our subsequent analysis to the ERA-Interim dataset, recalling its denser global coverage compared to the HadISDH.

As RH is mostly dependent on changes in specific humidity (q), there is a dominant high correlation between the interannual variability of RH and q (Supplementary Figure 5). In accordance, the magnitude of observed change in these two variables showed a strong agreement for 1979-2014. Figure 4 summarizes the magnitude of change in specific humidity (q) as well as changes in specific humidity necessary to maintain RH constant as recorded in 1979. Specific humidity showed the strongest decrease in Southwest North America, the Amazonian region, Southern South America and the Sahel regions: a spatial pattern that is similar to RH pattern. Given the evolution of air temperature between for 1979-2014, these regions exhibited a deficit of water vapor on the order of -2 g/kg^{-1} in order to maintain RH constant.

3.2. Spatial patterns of the dependency between RH and climate variables

Based on the high agreement between the HadISDH and the ERA-Interim datasets in reproducing consistent seasonal and annual trends in RH, we selected a range of regions (N=14) worldwide (Figure 5). For these selected regions, we assessed the connection between RH and some relevant climatic variables for the period 1979-2014. In addition, we defined the oceanic and continental sources of moisture corresponding to these regions using the FLEXPART model. We assessed the optimal lifetime for each region: during 4 days in back for regions 1-5 and 7-11, during 5 days for regions 6, 12-13, and during 7 days for region 5 (see section 2.2). Figures 6-8 show some examples of the dependency between RH and different climate variables at the annual scale. Results for all regions at the seasonal and annual scales are presented in supplementary materials.

<u>3.2.1. West Sahel</u>

Figure 6 (top) illustrates RH trends in the West Sahel using the HadISDH and ERA-Interim datasets. We also showed the distribution of the average annual moisture sources (E-P in mm) over this region for 1979-2014. As illustrated, the atmospheric moisture is mostly coming from the western Sahel region itself, in addition to some oceanic sources located in the central eastern Atlantic Ocean. At the seasonal scale, there are some differences in the location and the intensity of the moisture sources, with more oceanic contribution during the boreal warm season. However, in both cases, the continental moisture seems to be the key source of humidity in the region (Suppl. Figures 21 and 35). In other areas, e.g. the Western European region (Suppl. Figures 17 and 31), we observed marked differences in the location and the intensity of humidity sources between the boreal cold and warm seasons. Figure 6 (central) shows different scatterplots summarizing the relationships between the de-trended annual series of RH and those of relevant climate variables (e.g. precipitation, air temperature and SST). As illustrated, the interannual variability of RH in the region is correlated to changes in the total annual precipitation and the total annual land evapotranspiration in the continental source region. Specifically, the correlation between the de-trended annual RH and precipitation and land evapotranspiration is generally above 0.8 ($p < 0.05$). In contrast, RH shows negative correlations with air temperature and SST ratio over the oceanic source. While the correlation is statistically insignificant ($p>0.05$), it suggests that higher differences between air temperature and SST reinforce lower annual RH. At the seasonal scale, we found similar patterns (Supplementary Figs. 21 and 35), with RH being highly correlated with land evapotranspiration during the boreal cold and warm seasons. Nevertheless, in the warm season, a significant negative correlation with air temperature and SST ratio was observed. This pattern concurs with the significant increase in specific humidity (q) for 1979-2014; this is probably related to the high increase in land evapotranspiration (19.5%, $p < 0.05$).

<u>3.2.2. La Plata region</u>

Figure 7 summarizes the corresponding results, but for La Plata region (South America). Results indicate a general decrease in RH at the annual and seasonal scales using both the HadISDH observational data and the ERA-Interim dataset. As depicted, the main humidity sources are located in the same region, combined with some other continental neighbor areas over South America. A similar finding was also observed at the seasonal scale (Supplementary Figs. 25 and 39). Similar to the West Sahel region, we found a significant association between the interannual variations of RH and precipitation and the land evapotranspiration in the continental source region. Similarly, we did not find any significant correlation between RH changes and the interannual variability of the oceanic evaporation in the oceanic source region as well as the ratio between air temperature in the continental target region and SST in the oceanic source region. Again, we found a negative correlation between RH and air temperature/SST ratio, though being statistically insignificant at the annual scale ($p>0.05$). In La Plata region, we noted a strong decrease in RH (-6.21%/decade) for 1979-2014, which agrees well with the strong decrease in absolute humidity. This region is strongly impacted by continental atmospheric moisture sources, with a general decrease in precipitation and land evapotranspiration during the analyzed period.

3.2.3. Southwest North America

Results for Southwest North America are also illustrated in Figure 8. In accordance with both previous studied examples (West Sahel and La Plata), this region also exhibited a strong and positive relationship between the interannual variability of RH and precipitation and land evapotranspiration. This pattern was also recorded for the boreal warm and cold seasons (Supplementary Figures 28 and 42). In this region, we found a strong negative trend of RH for 1979-2014, which concurs with the significant decrease of absolute humidity. We noted a significant increase in air temperature, air temperature and air temperature to SST ratio, while a negative and statistically significant decrease in land evapotranspiration in the continental sources of moisture was observed.

3.2.4. Other regions

Other regions of the world (see Supplementary Material) also showed strong dependency between the interannual variability of RH and that of land evapotranspiration in the land moisture sources. Some examples include Western Europe, Central-eastern Europe, Southeast Europe, Turkey, India and the east Sahel. Nevertheless, the influence of land evapotranspiration was very different between the boreal warm and cold seasons (e.g. Scandinavia, Central-east Europe and the Amazonian region). In contrast, other regions showed a weak correlation between the temporal variability of RH and land evapotranspiration in the moisture source region. A representative example is China, which witnessed a strong decrease in RH for 1979-2014. This might be explained largely by the fact that relative interannual ET variations are just much weaker in China compared to other regions so that the signal-to-noise ratio is worse in China. In this region, RH changes correlated significantly with annual precipitation only: a variable that did not show significant changes from 1979 to 2014 (Supplementary Fig. 11). This annual pattern was also observed for the boreal cold and warm seasons (Supplementary Figs. 23 and 37).

Nevertheless, although the interannual variability of land evapotranspiration in the land moisture sources showed the highest correlation with RH variability in the majority of the analyzed regions, air temperature/SST ratio in the oceanic moisture sources also exhibited negative correlations with RH in particular regions, including West Sahel, La Plata, West Coast of the USA, Central-eastern Europe, India, central North America and the Amazonian region. This finding suggests that higher differences between air temperature in the target area and SST in the oceanic moisture region would favor decreased RH.

In summary, changes in RH were mostly associated with the observed changes in land evapotranspiration across the selected regions (Figure 9). In contrast, annual changes in RH did not correlate significantly with precipitation, air temperature/SST and oceanic evaporation. For the boreal warm and cold seasons we found a similar pattern (Supplementary Figs. 45 and 46).

3.3. Global relationship between RH and land evapotranspiration

Figure 10 depicts the relationship between RH and land evapotranspiration seasonally and annually at the global scale. Note that these are local ("pixel-by-pixel") correlations and the interpretation differs from the previous analysis where RH in target regions is correlated with ET in corresponding source regions. Results reveal strong positive and significant correlations in large areas of the world. The strongest positive correlations were found in Central, West and Southwest North America, Argentina, east Brazil, South Africa, the Sahel, central Asia and the majority of Australia. Nevertheless, there are some exceptions, including large areas of the Amazon, China, central Africa and the high latitudes of the Northern Hemisphere, where the correlations were negative. In general, the areas with positive and significant correlations between RH and land evapotranspiration corresponded to those areas characterized by semiarid and arid climate characteristics, combined with some humid areas (e.g. India and northwest North America).

Overall, the global trends in land evapotranspiration were spatially coherent with those observed for RH. Figure 11 illustrates the spatial distribution of the magnitude of change in annual and seasonal land evapotranspiration at the global scale from 1979 to 2014. As depicted, the spatial patterns of land evapotranspiration changes resemble those of RH (refer to Figure 1). For example, a positive trend in the annual land evapotranspiration dominated over the Canadian region, which agrees well with the general increase in RH across the region. On the other hand, there was a dominant decrease in the annual land evapotranspiration across vast areas of North America, which concurs also with the strong decrease in RH. Similar to the pattern observed for land evapotranspiration, RH increased particularly over southwest North America. In South America, both variables also showed a dominant negative trend at the annual scale, but with some spatial divergences, mainly in the Amazonian region. Specifically, the western part of the basin showed the most important decrease in land evapotranspiration, whereas the most significant decrease in RH was observed in the eastern part. In the African continent, some areas showed good agreement between RH and land evapotranspiration changes, in terms of both the sign and magnitude. This can be clearly seen in the West and East Sahel, where a strong gradient in RH trend between the West (positive) and the East (negative) was observed. A similar pattern was also observed for the Namibia-Botswana-Angola region. Nevertheless, other African regions showed a divergent pattern between both variables. One example is the Guinea Gulf in Nigeria and Cameroon, where we noted a strong increase in land evapotranspiration, as opposed to RH changes. In Australia, although both variables showed a dominant positive trend, they did not match exactly in terms of the spatial pattern of the magnitude of change. This is particularly because the main increase in RH was found in the south, while the main increase in land evapotranspiration was noted in the north of the Continent. The Eurasian continent showed the main divergences between both variables. In the high latitudes of the continent, there was a dominant increase in both variables. For other regions (e.g. Western Europe), we noted a dominant RH decrease, which was not observed for land evapotranspiration. A similar pattern was observed over east China, with a dominant RH negative trend and a positive land evapotranspiration.

In any case, attributing causality to the observed RH changes is quite complex given divergences found at the global scale. We have computed the fraction of continentally-originated humidity for each region and season and related this fraction to the strength of the agreement between RH and Land evapotranspiration at the annual and seasonal scales. Supplementary Table 1 shows the percentage of contribution of continental areas to the total moisture in each one of the fourteen analyzed regions, which oscillate between 31.6% for West Europe and 64% in Northeast Asia. There is not a significant relationship between these percentages of contribution and the strength of the agreement between RH and land evapotranspiration obtained in each region (Supplementary Figure 47). This reinforces the complexity of attributing changes of RH to a single factor. In any case, in some of the regions that show significant changes in RH have been identified, there are also changes in the total contribution from continental areas at the seasonal and annual scales (Supplementary Figures 48-50). Both West Sahel and East Sahel show increased contribution of continental areas. On the other hand, La Plata region, in which there is also a strong agreement between RH and land evapotranspiration and that shows a significant negative trend in both variables, there is a decrease of the continental contribution. This stresses the complexity of giving a unique attribution to the observed RH changes.

In relation to the influence of the ocean evaporation, our results confirm that the global connection between oceanic evaporation and changes in RH is complex. On one hand, it is difficult to establish a pixel per pixel relationship since the sources of moisture may strongly differ at the global scale. On the other hand, it is not feasible to identify moisture sources for each 0.5º pixel at the global scale. However, we believe that the analysis of the evolution of SST and oceanic evaporation for 1979-2014 can give indications on some relevant patterns. Figure 12 illustrates the spatial distribution of the magnitude of change of annual and seasonal SST and oceanic evaporation. Supplementary Fig. 51 shows the spatial distribution of trend significance. As depicted, complex spatial patterns and high variability of the trends were observed, particularly for oceanic evaporation. Furthermore, the spatial distribution of the magnitude of change in annual and seasonal oceanic evaporation was not related to the SST changes (Supplementary Fig. 52). This finding suggests that oceanic evaporation is not only driven by changes in SST. Thus, although some regions showed positive changes in the oceanic evaporation, the amount of increase was much lower than that found for SST, which suggests that only SST changes do not drive evaporation changes (Supplementary Figure 53, Supplementary Table 2).

4. Discussion

We assessed the temporal variability and trends of relative humidity (RH) at the global scale using a dense observational network of meteorological stations (HadISDH) and reanalysis data (ERA-Interim). Results revealed high agreement of the interannual variability of RH using both datasets for 1979-2014. This finding was also confirmed, even for the regions where the density of the HadISDH observatories was quite poor (e.g. the northern latitudes and tropical and equatorial regions). Recent studies have suggested dominant decrease in observed RH during the last decade (e.g. Simmons et al., 2010; Willet et al., 2014). Our study suggests dominant negative trends of RH using the HadISDH dataset. This decrease is mostly linked to the temporal evolution of RH during the boreal warm season. Nevertheless, other regions showed positive RH trends. In accordance with the HadISDH dataset, the ERA-Interim revealed dominant negative

RH trends, albeit with a lower percentage of the total land surface compared to the HadISDH dataset. These differences cannot be attributed to the selected datasets, given that both mostly agree on the magnitude and sign of changes in RH.

Observed changes in RH were closely related to the magnitude and the spatial patterns of specific humidity changes. Results demonstrate a general deficit of specific humidity to maintain RH constant in large areas of the world, including the central and south Northern America, the Amazonas and La Plata basins in South America and the East Sahel. In other regions, RH increased in accordance with higher specific humidity. Some studies suggested that changes in air temperature could partly cancel the effects of the atmospheric humidity to explain RH changes (e.g. McCarthy and Tuomi, 2004; Wright et al., 2010; Sherwood, 2010). Nevertheless, although air temperature trends showed spatial differences at the global scale over the past four decades (IPCC, 2013), our results confirm that air temperature is not the main driver of the observed changes of RH globally. The ERA-Interim dataset clearly showed a close resemblance between RH and specific humidity trends at the global scale. This suggests that specific humidity is the main driver of the observed changes in the magnitude and spatial pattern of RH during the past decades.

Overall, there is a strong agreement between the interannual variability of precipitation and land evapotranspiration in the continental moisture source and the interannual variability of RH in the different regions. Moreover, we found a close spatial relationship between RH changes over each of these regions and the observed changes in precipitation and land evapotranspiration over the continental source regions. Land evapotranspiration is also closely related to precipitation variability, so increased land evapotranspiration tends to be caused primarily by increased precipitation, which is accompanied by corresponding RH anomalies. These findings suggest that, at the annual and seasonal scales, the interannual variability of land evapotranspiration was significantly correlated with RH changes over most of the continental areas. However, this finding should be seen in the context that RH at each site cannot be determined only by the land/water supply from the site itself, but it can further be controlled by land evapotranspiration over remote continental areas.

In general, our results suggest an influence of land-atmosphere water feedbacks and recycling processes on RH variability and trends. This is simply because more available soil humidity under favorable atmospheric and land conditions would result in more evapotranspiration and accordingly higher air moisture (Eltahir and Bras, 1996; Domínguez et al., 2006; Kunstmann and Jung, 2007). Recalling that the ocean surface evaporates about 84% of the water evaporated over the Earth (Oki, 2005), the oceanic evaporation is highly important for continental precipitation (Gimeno et al., 2010). However, the continental humidity sources can also be important. Numerous model-based studies have supported the strong influence of land evaporation processes on air humidity and precipitation over land surfaces (e.g. Bosilovich and Chern, 2006; Dirmeyer et al., 2009; Goessling and Reick, 2011). Moisture recycling is strongly important in some regions of the world, such as China and central Asia, the western part of Africa and the central South America (Pfahl et al., 2014; van der Ent et al., 2010). In Europe, Ruosteenoja and Raisanen (2013) linked RH variability to some meteorological variables (e.g. air temperature, precipitation) in the Coupled Model Intercomparison Project Phase 3 (CMIP3) models. They indicated that seasons with anomalously large precipitation, which supply moisture to soils, are likely to coincide with anomalous RH, particularly in Northern Europe. They also concluded that an earlier springtime drying of soil in future will suppress evapotranspiration and further reduce RH over land. Similarly, Rowell and Jones (2006) analyzed different hypotheses to explain the projected summer drying conditions in Europe, suggesting that soil moisture decline and land–sea contrast in lower tropospheric summer could be the key factors responsible for this drying. They concluded that reduced evaporation in summer will drop RH and hence reduced continental rainfall. These would impact soil moisture and evapotranspiration processes, inducing a reduction in RH and rainfall, through a range of atmospheric feedbacks. In the same context, the importance of moisture recycling processes for atmospheric humidity and precipitation has been recently identified in semi-arid and desert areas of the world (Miralles et al., 2016).

Although our study was limited to specific regions across the world, results indicate that humidity in the analyzed regions is largely originated over continental rather than oceanic areas. This finding concurs with some regional studies that defined sources of moisture (e.g., Nieto et al., 2014; Gimeno et al., 2010; Drumond et al., 2014; Ciric et al., 2016). Also, our results suggest a strong association between land evapotranspiration and RH variability, which could stres the importance of humidity recycling processes for explaining RH variability over continental areas.

In contrast to the general high correlations found between the interannual variability of RH and land evaporation, the ratio between air temperature and SST in the source region did not show significant correlations with RH changes, albeit with the dominant positive trend found for this ratio in the majority of the analyzed regions. Different modelled climate studies suggested strong differences between land and ocean RH trends, as a consequence of the different warming rates between oceanic and continental areas (e.g. Joshi et al., 2008; Dessler and Sherwood, 2009; O'Gorman and Muller, 2010). As the warming rates are generally slower over oceans, the specific humidity of air advected from oceans to continents would increase more slowly than the saturation specific humidity over land, causing a reduction in RH (Rowell and Jones 2006). Due to this effect, RH will not remain constant in areas located very far from humidity sources, as warmer air temperatures under limited moisture humidity would reduce RH (Pierce et al., 2013). Recalling the observed negative RH trend at many coastal regions over the period 1979-2014, this study confirms that the distance to oceanic humidity sources is not a key controller of the spatial patterns of RH changes. In many instances, we found that continental regions, which are very far from oceans (e.g. Canada, central China and Kazakhstan), recorded a positive RH trend. This finding indicates that while different model experiments fully supported the hypothesis that the different warming rates between oceanic and continental areas can explain the projected decrease in RH under climate change conditions, our results for 14 different regions in the world show a non-clear influence of the air temperature to SST ratio to explain the observed RH trends. A possible explanation of these contrasting findings is related to the low differences in the warming rates between the oceanic sources and continental target areas. We found that -in most of the cases- these differences were not strong enough to generate a clear effect at the global scale, particularly with the available number of observations. The dominant negative correlation between RH and air temperature/SST in the analyzed regions, though being weak, seems to support this finding.

Also, we did not find a significant relationship between the interannual variability of the oceanic evaporation in the oceanic humidity source regions and RH in the target areas, both at annual and seasonal scales. Although oceanic evaporation is decisive on continental evaporation (Gimeno et al., 2010), current trends in RH are not related to the observed oceanic evaporation trends over the humidity source areas. In accordance with previous studies (e.g. Rayner et al., 2003; Deser et al., 2010), we found a general SST increase in the oceanic areas at the global scale, albeit with some spatial exceptions. Nevertheless, this increase does not imply that oceanic evaporation increased at the same rate as SST. Here, we indicated that oceanic evaporation trends for 1979-2014 showed strong spatial variability at the global scale, with dominant positive trends. Nevertheless, large areas also exhibited insignificant trends and even negative evaporation trends. While SST increase is mainly associated with radiative processes, evaporation processes are mainly controlled by a wide range of meteorological variables that impact the aerodynamic and radiative components of the atmospheric evaporative demand (AED) rather than SST alone (McVicar et al., 2012b). This is consistent with the finding that global mean precipitation or evaporation does not scale with Clausius–Clapeyron (Held and Soden 2006). Due to the unlimited water availability over oceans, air vapor pressure deficit is expected to be driven by the Clausius-Clapeyron relation. However, changes in solar radiation and wind speed can also influence the evaporation evolution (Yu, 2007; Kanemaru and Masunaga, 2013). As such, given the slow oceanic evaporation trends in large regions of the world, RH trends in the analyzed target regions can significantly be associated with oceanic evaporation. Nevertheless, changes in other variables could also explain the relatively small role of the oceanic moisture sources in RH variability and trends in the analyzed continental areas. In this work, we did not consider the "effectivity" of the oceanic moisture (Gimeno et al., 2012) because the water vapor evaporated over the oceanic regions could not reach the target region due to some geographical constraints (e.g. topography). Also, we did not analyze the transport mechanisms between the source and target areas. Moreover, moisture source regions are not stationary, as the intensity of humidity can vary greatly from one year to another (Gimeno et al., 2013). This aspect could be another source of uncertainty in the explanatory factors of current RH trends. Furthermore, other different factors that control atmospheric humidity and RH have not been approached in this study. Sherwood (1996) suggested that RH distributions are strongly controlled by dynamical fields rather than local air temperatures. This suggests that atmospheric circulation processes could largely affect the temporal variability and trends of RH. A range of studies indicates noticeable changes in RH, in response to low-frequency atmospheric oscillations, such as the Atlantic Multidecadal Oscillation (AMO) and El Niño-Southern Oscillation (e.g. McCarthy and Toumi, 2004; Zhang et al., 2013), as well as changes in the Hadley Cell (HC) (Hu and Fu, 2007). Wright et al. (2010) employed a global climate model under double CO_2 concentrations to show that tropical and subtropical RH is largely dependent on a poleward expansion of the Hadley cell: a deepening of the height of convective detrainment, a poleward shift of the extratropical jets, and an increase in the height of the tropopause. Also, Laua and Kim (2015) assessed changes in the HC under CO_2 warming from the Coupled Model Intercomparison Project Phase-5 (CMIP5 model projections. They suggest that strengthening of the HC induces atmospheric moisture divergence and reduces tropospheric RH in the tropics and subtropics. This spatial pattern resembles the main areas showing negative trends in RH in our analysis.

Here, we found that actual evapotranspiration processes from the continental humidity sources can be relevant to explain recent temporal variability and trends of RH. Overall, the proposed mechanisms by Sherwood and Fu (2014) of increased aridity by enhanced AED driven by lower RH under a climate change scenario is fully valid, regardless of which factors cause the reduction of RH. Seneviratne et al. (2002) used a regional climate model, combined with a land-surface scheme of intermediate complexity, to investigate the sensitivity of summer climate to enhanced greenhouse warming over the American Midwest. They indicated that vegetation control on transpiration might play an important part in counteracting an enhancement of summer drying, particularly when soil water gets limited. Other studies provide similar results in other regions using both observational data (e.g. Hisrchi et al., 2011) and model outputs (e.g. Seneviratne et al., 2006; Fischer et al., 2007). Therefore, the aridification processes would be even more severe if the suppression of the land evapotranspiration is the main driver of RH reduction. Also, the AED can increase, particularly when enhanced air dryness is driven by soil moisture dryness, inducing an increase in aridity and the severity of drought episodes.

5. Conclusions

The main conclusions of this study are:

- There are dominant negative trends of RH and this decrease is mostly linked to the temporal evolution of RH during the boreal warm season. Negative trends do not show homogeneous spatial patterns, and some regions also show positive trends.
- There is a high agreement between RH and specific humidity trends at the global scale, suggesting a moisture deficit in large areas to explain RH trends in opposition to atmospheric warming.
- In general we found significant correlations between the interannual variability of land evapotranspiration and RH.
- There are not correlation between the ratio of the air temperature over the target regions and SST in the source regions and the RH variability.
- There is not a significant relationship between the interannual variability of the oceanic evaporation in the oceanic humidity source regions and RH in the target areas.

Given strong relevance of understanding current RH trends at the global scale, further research is still needed to consider other dynamic and radiative factors that may affect the temporal variability and trends of RH over continental regions.

Acknowledgements

This work was supported by the EPhysLab (UVIGO-CSIC Associated Unit), PCIN-2015-220, CGL2014-52135-C03-01, CGL2014-60849-JIN, *Red de variabilidad y cambio climático* RECLIM (CGL2014-517221-REDT) financed by the Spanish Commission of Science and Technology and FEDER, and IMDROFLOOD financed by the Water Works 2014 co-funded call of the European Commission.

References

Berg, A., Findell, K., Lintner, B., et al.: Land-atmosphere feedbacks amplify aridity increase over land under global warming, Nature Climate Change, 6, 869-874, 2016.

Bosilovich, M.G., Chern, J.-D.: Simulation of water sources and precipitation recycling for the MacKenzie, Mississippi, and Amazon River basins, Journal of Hydrometeorology, 7, 312-329, 2006.

Byrne, M.P., O'Gorman, P.A.: Link between land-ocean warming contrasts and surface relative humidities in simmulations with coupled climate models, Geophysical Research Letters, 40, 5223-5227, 2013.

Buck, A. L.: New equations for computing vapor pressure and enhancement factor, J. Appl. Meteorol., 20, 1527–1532, 1981.

Ciric, D., Stojanovic, M., Drumond, A., Nieto, R., Gimeno, L.: Tracking the origin of moisture over the danube river basin using a Lagrangian approach. Atmosphere, 7, 162, 2016.

Dai, A.: Recent climatology, variability, and trends in global surface humidity. J Clim, 19, 3589–3606, 2006.

Dee, D. P., Uppala, S. M., Simmons, A. J. et al.: The ERA-Interim reanalysis: configuration and performance of the data assimilation system, Q. J. R. Meteorol. Soc., 137, 553–597, 2011.

Deser, C., Phillips, A.S., Alexander, M.A.: Twentieth century tropical sea surface temperature trends revisited, Geophysical Research Letters, 37, L10701, 2010.

Dessler, A. E., Sherwood, S. C.: Atmospheric Science: A Matter of Humidity, Science, 323, 1020–1021, 2009.

Dirmeyer, P.A., Schlosser, C.A., Brubaker, K.L.: Precipitation, recycling, and land memory: An integrated analysis, Journal of Hydrometeorology, 10, 278-288, 2009.

Dominguez, F., Kumar, P. Liang, X., Ting, M.: Impact of atmospheric moisture storage on precipitation recycling, J. Clim., 19, 1513–1530, 2006.

Drumond, A., Marengo, J., Ambrizzi, T. et al.: The role of the Amazon Basin moisture in the atmospheric branch of the hydrological cycle: A Lagrangian analysis, Hydrology and Earth System Sciences, 18, 2577-2598, 2014.

Eltahir, E.A.B., Bras, R.L.: Precipitation recycling, Reviews of Geophysics, 34, 367-378, 1996.

Fan, Z.-X., Thomas, A.: Spatiotemporal variability of reference evapotranspiration and its contributing climatic factors in Yunnan Province, SW China, 1961-2004, Climatic Change, 116, 309-325, 2013.

Ferraro, A.J., Lambert, F.H., Collins, M., Miles, G.M.: Physical mechanisms of tropical climate feedbacks investigated using temperature and moisture trends. Journal of Climate, 28, 8968-8987, 2015.

Fischer, E.M., Seneviratne, S.I., Vidale, P.L., Lüthi, D., Schär, C.: Soil moisture-atmosphere interactions during the 2003 European summer heat wave, Journal of Climate, 20, 5081-5099, 2007.

Gimeno, L., Nieto, R., Trigo, R.M., Vicente-Serrano, S.M., López-Moreno, J.I.: Where does the Iberian Peninsula moisture come from? An answer based on a Lagrangian approach, Journal of Hydrometeorology, 11, 421-436, 2010.

Gimeno, L., Stohl, A., Trigo, R.M., et al.: Oceanic and terrestrial sources of continental precipitation, Reviews of Geophysics, 50, RG4003, 2012.

Gimeno, L., Nieto, R., Drumond, A., Castillo, R., Trigo, R.: Influence of the intensification of the major oceanic moisture sources on continental precipitation, Geophysical Research Letters, 40, 1443-1450, 2013.

Goessling, H.F. and Reick, C.H., 2011. What do moisture recycling estimates tell us? Exploring the extreme case of non-evaporating continents. Hydrology and Earth System Sciences, 15, pp.3217-3235.

Hamed, K. H., Rao, A. R.: A modified Mann Kendall trend test for autocorrelated data, J. Hydrol., 204, 182–196, 1998.

Harris, I., Jones, P.D., Osborn, T.J., Lister, D.H.: Updated high-resolution grids of monthly climatic observations – the CRU TS3.10 Dataset, International Journal of Climatology, 34, 623–642, 2014.

Held, I.M. and Soden, B.J., 2006. Robust responses of the hydrological cycle to global warming. Journal of Climate, 19: 5686-5699.

Hirschi, M., Seneviratne, S.I., Alexandrov, V. et al.: Observational evidence for soil-moisture impact on hot extremes in southeastern Europe, Nature Geoscience, 4, 17-21, 2011.

Hosseinzadeh Talaee, P., Sabziparvar, A.A., Tabari, H.: Observed changes in relative humidity and dew point temperature in coastal regions of Iran, Theoretical and Applied Climatology, 110, 385-393, 2012.

Hu, Y., Fu, Q.: Observed poleward expansion of the Hadley circulation since 1979, Atmospheric Chemistry and Physics, 7, 5229-5236, 2007.

IPCC: Climate Change 2013: The Physical Science Basis. Contribution of Working Group I to the Fifth Assessment Report of the Intergovernmental Panel on Climate Change [Stocker, T.F., D. Qin, G.-K. Plattner, M. Tignor, S.K. Allen, J. Boschung, A. Nauels, Y. Xia, V. Bex and P.M. Midgley (eds.)]. Cambridge University Press, Cambridge, United Kingdom and New York, NY, USA, 1535 pp, 2013.

Jensen, M. E., Burman, R. D., and Allen, R. G. (Eds.): Evapotranspiration and Irrigation Water Requirements: ASCE Manuals and Reports on Engineering Practices No. 70, American Society of Civil Engineers, New York, 360 pp., 1990.

Jhajharia, D., Shrivastava, S.K., Sarkar, D., Sarkar, S.: Temporal characteristics of pan evaporation trends under the humid conditions of northeast India, Agricultural and Forest Meteorology, 149, 763-770, 2009.

Joshi, M.M., Gregory, J.M., Webb, M.J., Sexton, D.M.H., Johns, T.C.: Mechanisms for the land/sea warming contrast exhibited by simulations of climate change, Climate Dynamics, 30, 455-465, 2008.

Kanemaru, K., Masunaga, H.: A satellite study of the relationship between sea surface temperature and column water vapor over tropical and subtropical oceans, Journal of Climate, 26, 4204-4218, 2013.

Kennedy J.J., Rayner, N.A., Smith, R.O., Saunby, M., Parker, D.E.: Reassessing biases and other uncertainties in sea-surface temperature observations since 1850 part 1: measurement and sampling errors, J. Geophys. Res., 116, D14103, 2011a.

Kennedy J.J., Rayner, N.A., Smith, R.O., Saunby, M. and Parker, D.E.: Reassessing biases and other uncertainties in sea-surface temperature observations since 1850 part 2: biases and homogenisation. J. Geophys. Res., 116, D14104, 2011b.

Kunstmann, H., Jung, G.: Influence of soil-moisture and land use change on precipitation in the volta basin of West Africa, International Journal of River Basin Management, 5, 9-16, 2007.

Lambert, F. H., Chiang, J.C.H.: Control of land-ocean temperature contrast by ocean heat uptake, Geophys. Res. Lett., 34, L13704, 2007.

Laua, W.K.M., Kim, K.-M.: Robust Hadley circulation changes and increasing global dryness due to CO2 warming from CMIP5 model projections. Proceedings of the National Academy of Sciences of the United States of America, 112, 3630-3635, 2015.

Lorenz, D.J., DeWeaver, E.T.: The response of the extratropical hydrological cycle to global warming, Journal of Climate, 20, 3470-3484, 2007.

Marengo, J.A., Nobre, C.A., Tomasella, J. et al.: The drought of Amazonia in 2005, Journal of Climate, 21, 495-516, 2008.

Martens, B., Miralles, D.G., Lievens, H., van der Schalie, R., de Jeu, R.A.M., Fernández-Prieto, D., Beck, H.E., Dorigo, W.A., and Verhoest, N.E.C.: GLEAM v3: satellite-based land evaporation and root-zone soil moisture, Geoscientific Model Development Discussions,

McCarthy, M.P., Toumi, R.: Observed interannual variability of tropical troposphere relative humidity, Journal of Climate, 17, 3181-3191, 2004.

McCarthy, M.P., Thorne, P.W., Titchner, H.A.: An analysis of tropospheric humidity trends from radiosondes, Journal of Climate, 22, 5820-5838, 2009.

McVicar, T.R., Roderick, M.L., Donohue, R.J., Van Niel, T.G.: Less bluster ahead? Ecohydrological implications of global trends of terrestrial near-surface wind speeds, Ecohydrology, 5, 381–388, 2012a.

McVicar, T.R., Roderick, M.L., Donohue, R.J., et al.: Global review and synthesis of trends in observed terrestrial near-surface wind speeds: implications for evaporation, J. Hydrol, 416–417, 182–205, 2012b.

Miralles, D.G., Holmes, T.R.H., de Jeu, R.A.M., Gash, J.H., Meesters, A.G.C.A., Dolman, A.J.: Global land-surface evaporation estimated from satellite-based observations, Hydrology and Earth System Sciences, 15, 453–469, 2011.

Miralles, D.G., Nieto, R., McDowell, N.G., Dorigo, W.A., Verhoest, N.E.C., Liu, Y.Y., Teuling, A.J., Dolman, A.J., Good, S.P., Gimeno, L.: Contribution of water-limited ecoregions to their own supply of rainfall, Environmental Research Letters, 11, 124007, 2016.

Nieto, R., Castillo, R., Drumond, A., Gimeno, L.: A catalog of moisture sources for continental climatic regions, Water Resources Research, 50, 5322-5328, 2014.

Numaguti, A.: Origin and recycling processes of precipitating water over the Eurasian continent: experiments using an atmospheric general circulation model. J. Geophys. Res. Atmos., 104, 1957-1972, 1999.

O'Gorman, P.A., Muller, C.J.: How closely do changes in surface and column water vapor follow Clausius-Clapeyron scaling in climate change simulations? Environmental Research Letters, 5, 025207, 2010.

Oki, T.: The hydrologic cycles and global circulation. Encyclopedia of Hydrological Sciences, 13-22. 2005.

Pfahl, S., Madonna, E., Boettcher, M., Joos, H., Wernli, H.: Warm conveyor belts in the ERA-Interim Dataset (1979-2010). Part II: Moisture origin and relevance for precipitation, Journal of Climate, 27, 27-40, 2014.

Pierce, D.W., Westerling, A.L., Oyler, J.: Future humidity trends over the western United States in the CMIP5 global climate models and variable infiltration capacity hydrological modeling system. Hydrology and Earth System Sciences, 17, 1833-1850, 2013.

Rayner, N.A., Parker, D.E., Horton, E.B. et al.: Global analyses of sea surface temperature, sea ice, and night marine air temperature since the late nineteenth

century. Journal of Geophysical Research D: Atmospheres, 108, ACL 2-1 - ACL 2-29, 2003.
Rebetez, M., Mayer, H., Dupont, O., et al.: Heat and drought 2003 in Europe: A climate synthesis, Annals of Forest Science, 63, 569-577, 2006.
Rodell, M., Beaudoing, H.K., L'Ecuyer, T.S. et al.: The observed state of the water cycle in the early twenty-first century, Journal of Climate, 28, 8289-8318, 2015.
Roderick, M., Farquhar, G.D.: The cause of decreased pan evaporation over the past 50 years. Science, 15, 1410–1411, 2002.
Rowell, D.P., Jones, R.G.: Causes and uncertainty of future summer drying over Europe, Climate Dynamics, 27, 281-299, 2006.
Ruosteenoja, K., Raisanen, P.: Seasonal changes in solar radiation and relative humidity in europe in response to global warming, Journal of Climate, 26, 2467-2481, 2013.
Seneviratne, S.I., Pal, J.S., Eltahir, E.A.B., Schar, C.: Summer dryness in a warmer climate: A process study with a regional climate model, Climate Dynamics, 20, 69-85, 2002.
Seneviratne, S.I., Lüthi, D., Litschi, M., Schär, C.: Land-atmosphere coupling and climate change in Europe, Nature, 443, 205-209, 2006.
Shenbin, C., Yunfeng, L., Thomas, A.: Climatic change on the Tibetan Plateau: Potential evapotranspiration trends from 1961-2000, Climatic Change, 76, 291-319, 2006.
Sherwood, S.C.: Maintenance of the free-tropospheric tropical water vapor distribution. Part I: Clear regime budget, Journal of Climate, 9, 2903-2918, 1996.
Sherwood, S.C.: Direct versus indirect effects of tropospheric humidity changes on the hydrologic cycle, Environmental Research Letters, 5, 025206, 2010.
Sherwood, S., Fu, Q.: A drier future?, Science, 343, 737–739, 2014.
Simmons, A.J., Willett, K.M., Jones, P.D., Thorne, P.W., Dee, D.P.: Low-frequency variations in surface atmospheric humidity, temperature, and precipitation: inferences from reanalyses and monthly gridded observational data sets. J. Geophys. Res .D Atmos., 115, D01110, 2010.
Stohl, A. and James, P.: A Lagrangian Analysis of the Atmospheric Branch of the GlobalWaterWater Cycle. Part I: Method Description, Validation and Demonstration for the August 2002 Flooding in Central Europe, J. Hydrometeorol., 5, 656–678, 2004.
Stohl, A., James, P.: A Lagrangian analysis of the atmospheric branch of the global water cycle. II. Moisture transports between Earth's ocean basins and river catchments, J. Hydrometeorol., 6, 961–984, 2005.
Trenberth, K.E., Fasullo, J., Smith, L.: Trends and variability in column-integrated atmospheric water vapor, Climate Dynamics, 24, 741-758, 2005.
Trenberth, K.E., Smith, L., Qian, T., Dai, A., Fasullo, J.: Estimates of the global water budget and its annual cycle using observational and model data, J. Hydrometeorol., 8, 758–769, 2007.
Van Der Ent, R.J., Savenije, H.H.G., Schaefli, B., Steele-Dunne, S.C. Origin and fate of atmospheric moisture over continents, Water Resources Research, 46, W09525, 2010.
Van Wijngaarden, W.A., Vincent, L.A.: Trends in relative humidity in Canada from 1953-2003, Bulletin of the American Meteorological Society, 4633-4636, 2004.
Vázquez, M., Nieto, R., Drumond, A., Gimeno, L.: Moisture transport into the Arctic: Source-receptor relationships and the roles of atmospheric circulation and

evaporation, Journal of Geophysical Research: Atmospheres, 121, 493-509, 2016.
Vicente-Serrano, S.M., Azorin-Molina, C., Sanchez-Lorenzo, A., Revuelto, J., Morán-Tejeda, E., López-Moreno, J.I., Espejo, F.: Sensitivity of reference evapotranspiration to changes in meteorological parameters in Spain (1961–2011), Water Resources Research, 50, 8458–8480, 2014a.
Vicente-Serrano, S.M., Azorin-Molina, C., Sanchez-Lorenzo, A., Morán-Tejeda, E., Lorenzo-Lacruz, J., Revuelto, J., López-Moreno, J.I., Espejo, F.: Temporal evolution of surface humidity in Spain: recent trends and possible physical mechanisms. Climate Dynamics, 42, 2655–2674, 2014b.
Vicente-Serrano, S.M., Azorin-Molina, C., Sanchez-Lorenzo, A., El Kenawy, A., Martín-Hernández, N., Peña-Gallardo, M., Beguería, S., Tomas-Burguera, M.: Recent changes and drivers of the atmospheric evaporative demand in the Canary Islands. Hydrology and Earth System Science, 20, 3393-3410, 2016.
Vincent, L.A., van Wijngaarden, W.A., Hopkinson, R.: Surface temperature and humidity trends in Canada for 1953-2005, Journal of Climate, 20, 5100-5113, 2007.
Wang, K., Dickinson, R.E.: A review of global terrestrial evapotranspiration: observation, modeling, climatology, and climatic variability, Rev. Geophys., 50, 2012.
Willett, K.M., Jones, P.D., Gillett, N.P., Thorne, P.W.: Recent changes in surface humidity: Development of the HadCRUH dataset, Journal of Climate, 21, 5364-5383, 2008.
Willett, K.M., Dunn, R.J.H., Thorne, P.W., Bell, S., de Podesta, M., Parker, D.E., Jones, P.D., Williams Jr., C.N.: HadISDH land surface multi-variable humidity and temperature record for climate monitoring, Clim. Past, 10, 1983-2006, 2014.
Wright, J.S., Sobel, A., Galewsky, J.: Diagnosis of relative humidity changes in a warmer climate, J. Clim., 23, 4556-4569, 2010.
Yu, L.: Global variations in oceanic evaporation (1958-2005): The role of the changing wind speed. J. Climate, 20, 5376–5390, 2007.
Yu, L., Jin, X., Weller, R.A.: Multidecade Global Flux Datasets from the Objectively Analyzed Air-sea Fluxes (OAFlux) Project: Latent and sensible heat fluxes, ocean evaporation, and related surface meteorological variables. Woods Hole Oceanographic Institution, OAFlux Project Technical Report. OA-2008-01, 64pp. Woods Hole. Massachusetts. 2008.
Yue, S., Wang, C.: The Mann-Kendall Test Modified by Effective Sample Size to Detect Trend in Serially Correlated Hydrological Series, Water Resour. Manage., 18, 201–218, 2004.
Zhang, X., Harvey, K. D., Hogg,W. D., and Yuzyk, T. R.: Trends in Canadian streamflow, Water Resour. Res., 37, 987–998, 2001.
Zhang, L., Wu, L., Gan, B.: Modes and mechanisms of global water vapor variability over the twentieth century, Journal of Climate, 26, 5578-5593, 2013.
Zongxing, L., Qi, F., Wei, L., Tingting, W., Yan, G., Yamin, W., Aifang, C., Jianguo, L., Li, L.: Spatial and temporal trend of potential evapotranspiration and related driving forces in Southwestern China, during 1961-2009, Quaternary International, 336, 127-144, 2014.

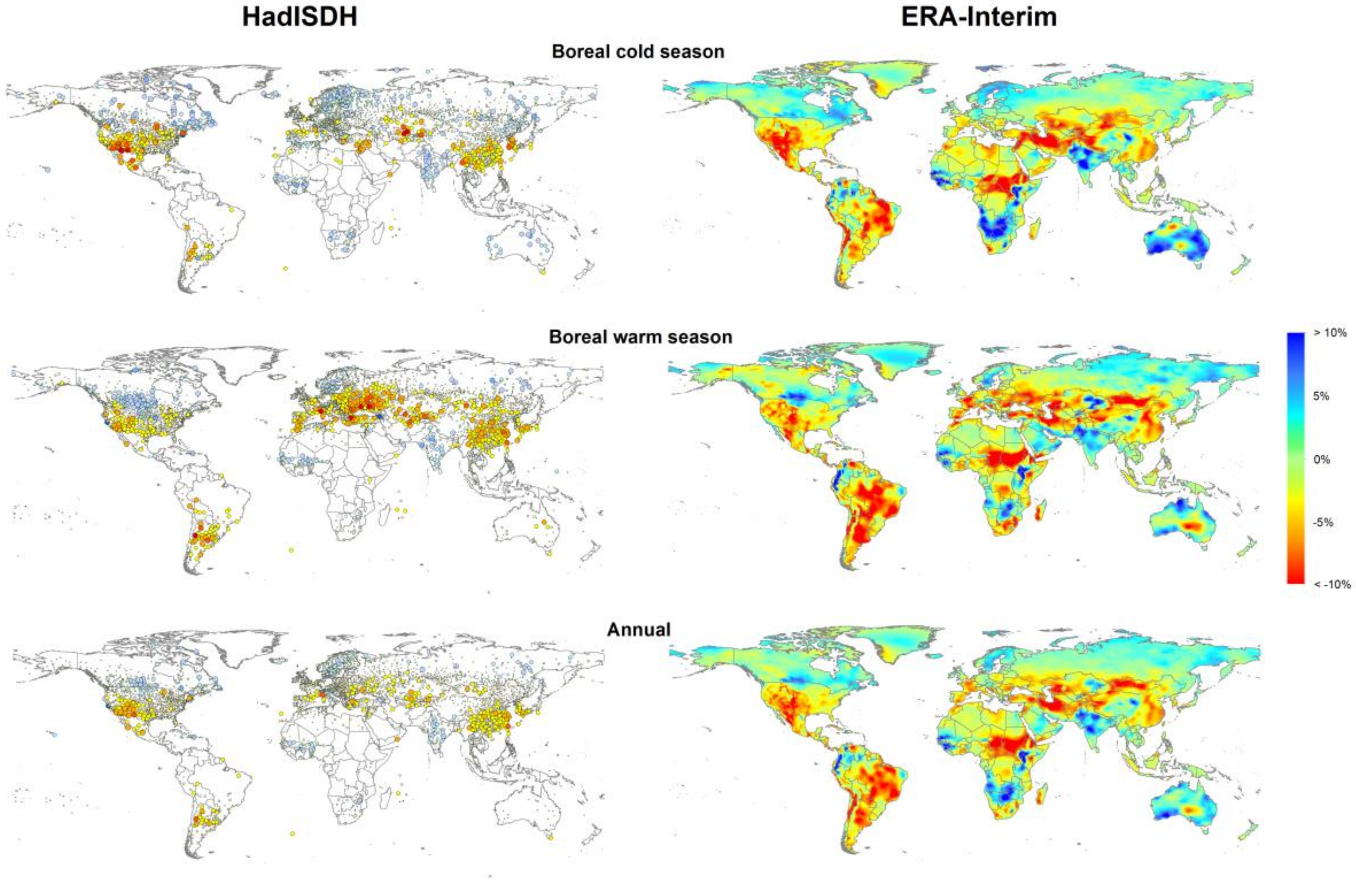

Figure 1. Spatial distribution of the magnitude of change of RH (% per decade) over the period 1979-2014 from HadISDH (left) and ERA-Interim dataset (right). Results are provided for the boreal cold (October-March) and warm (April-September) seasons and annually.

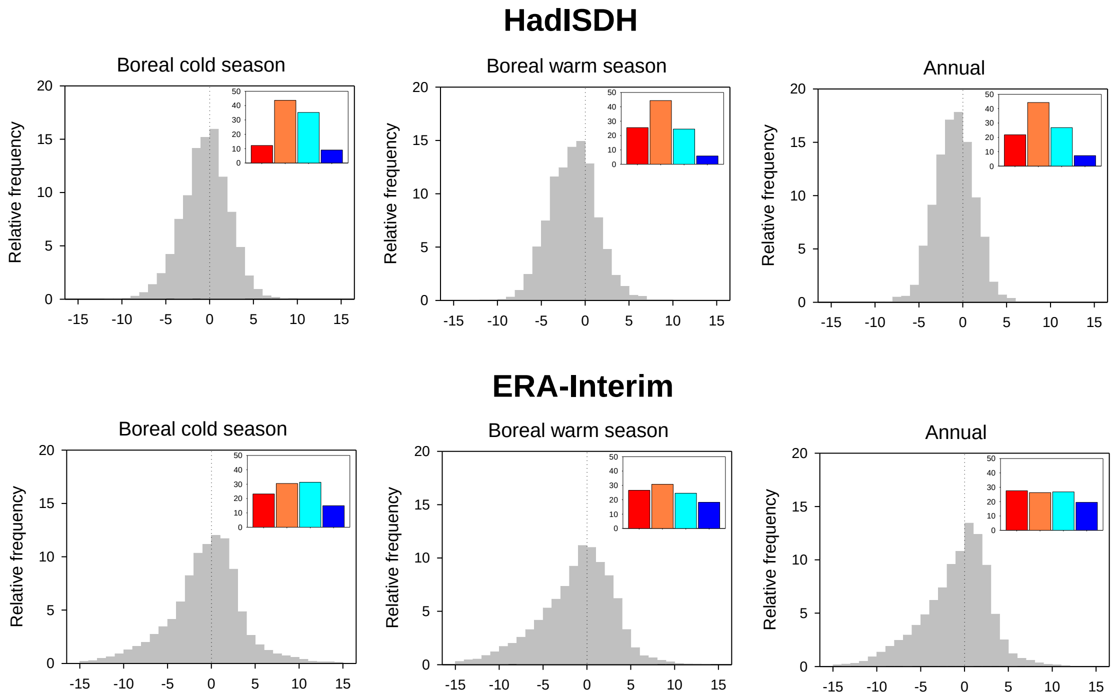

Figure 2: Relative frequencies (%) of the RH magnitude of change in the HadISDH and ERA-Interim datasets. Color bar plots represent the percentage of stations (from HadISDH) and world regions (from ERA-Interim) with positive and significant ($p < 0.05$) trends (blue), positive insignificant trends (cyan), negative insignificant trends (orange) and negative and significant trends (red).

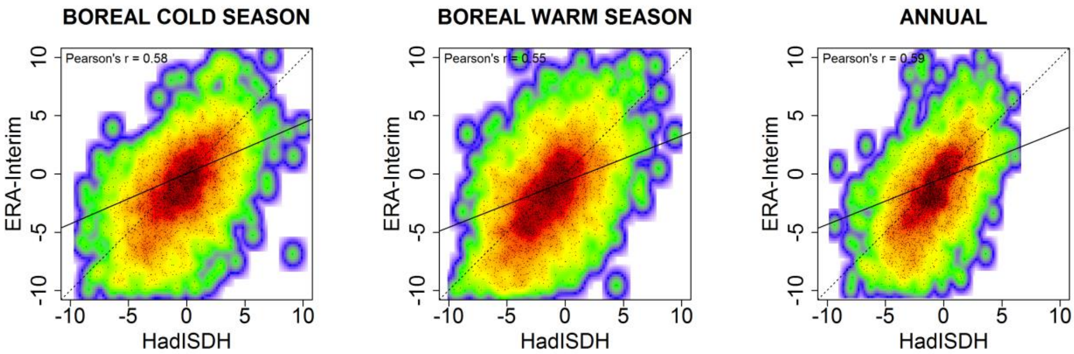

Figure 3: Scatterplots showing the global relationship between the magnitude of change in RH with HadISDH stations and ERA-Interim dataset at the seasonal and annual scales. Colors represent the density of points, with red color showing the highest density of points.

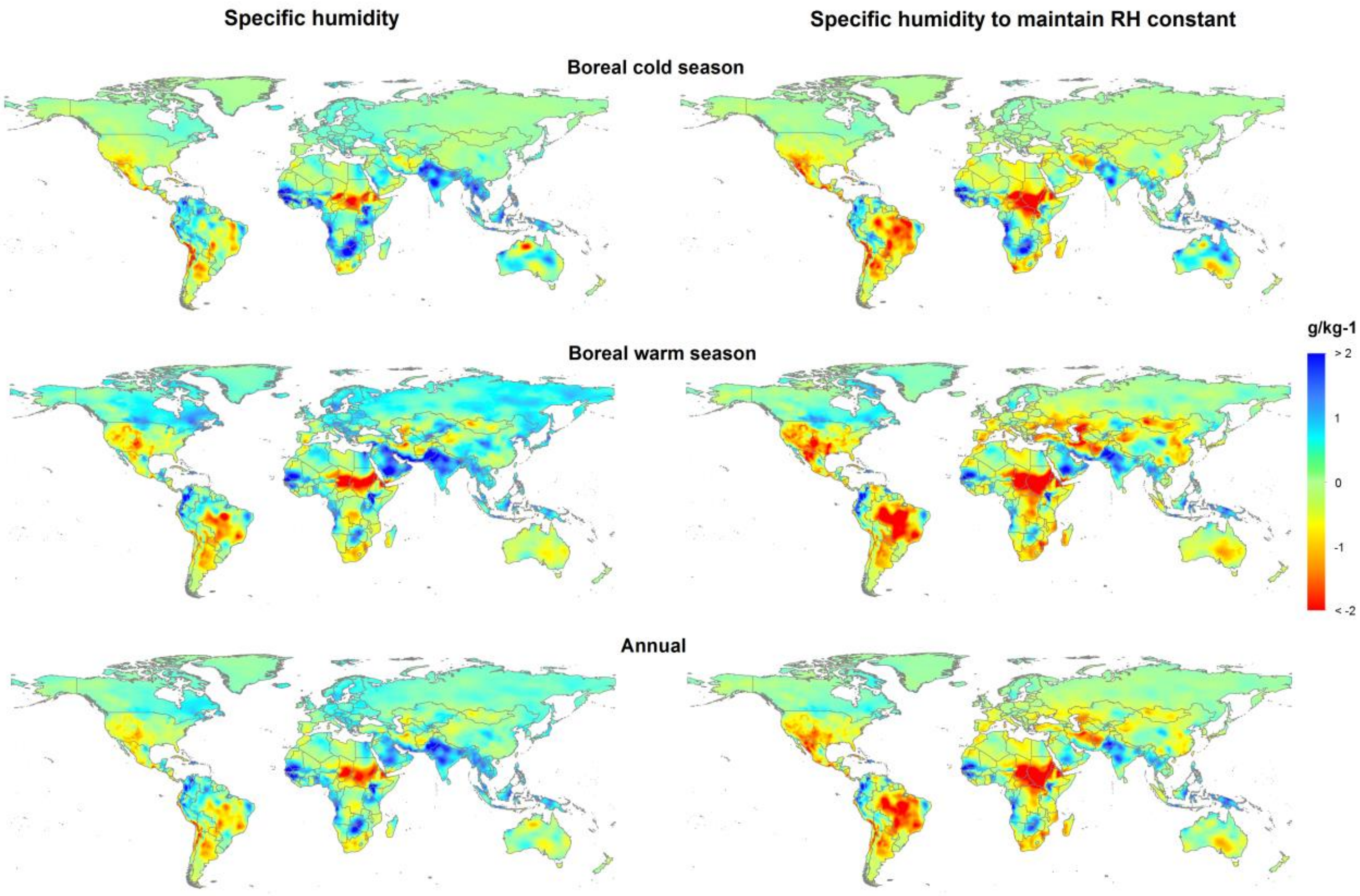

Figure 4: Spatial distribution of the seasonal and annual magnitudes of change in specific humidity (g/kg^{-1}) (left) and the deficit/surplus of specific humidity to maintain the RH constant with the levels of 1979 according to the land air temperature evolution (from the CRU TS v.3.23 dataset) for 1979-2014.

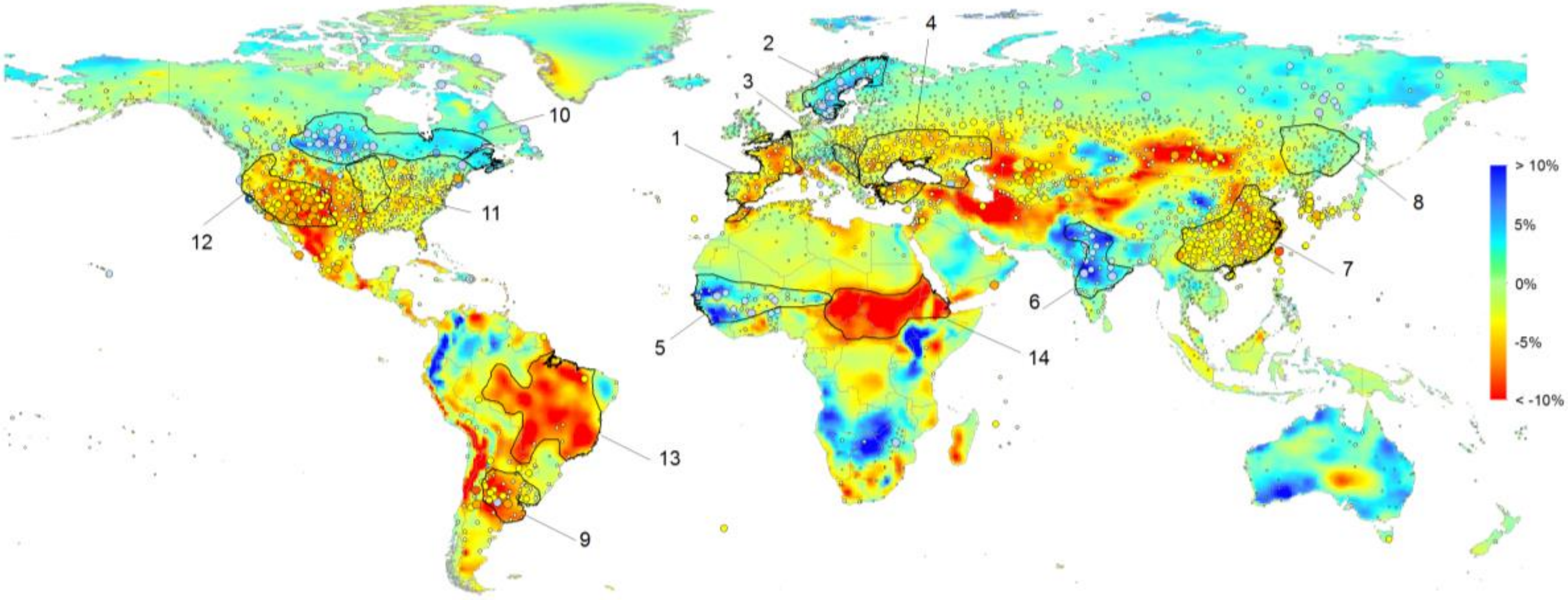

Figure 5: Distribution of the 14 world regions, with high consistency in RH trends between the HadISDH and the ERA-Interim datasets. These regions were selected for the identification of the oceanic and land humidity sources by means of the FLEXPART scheme.

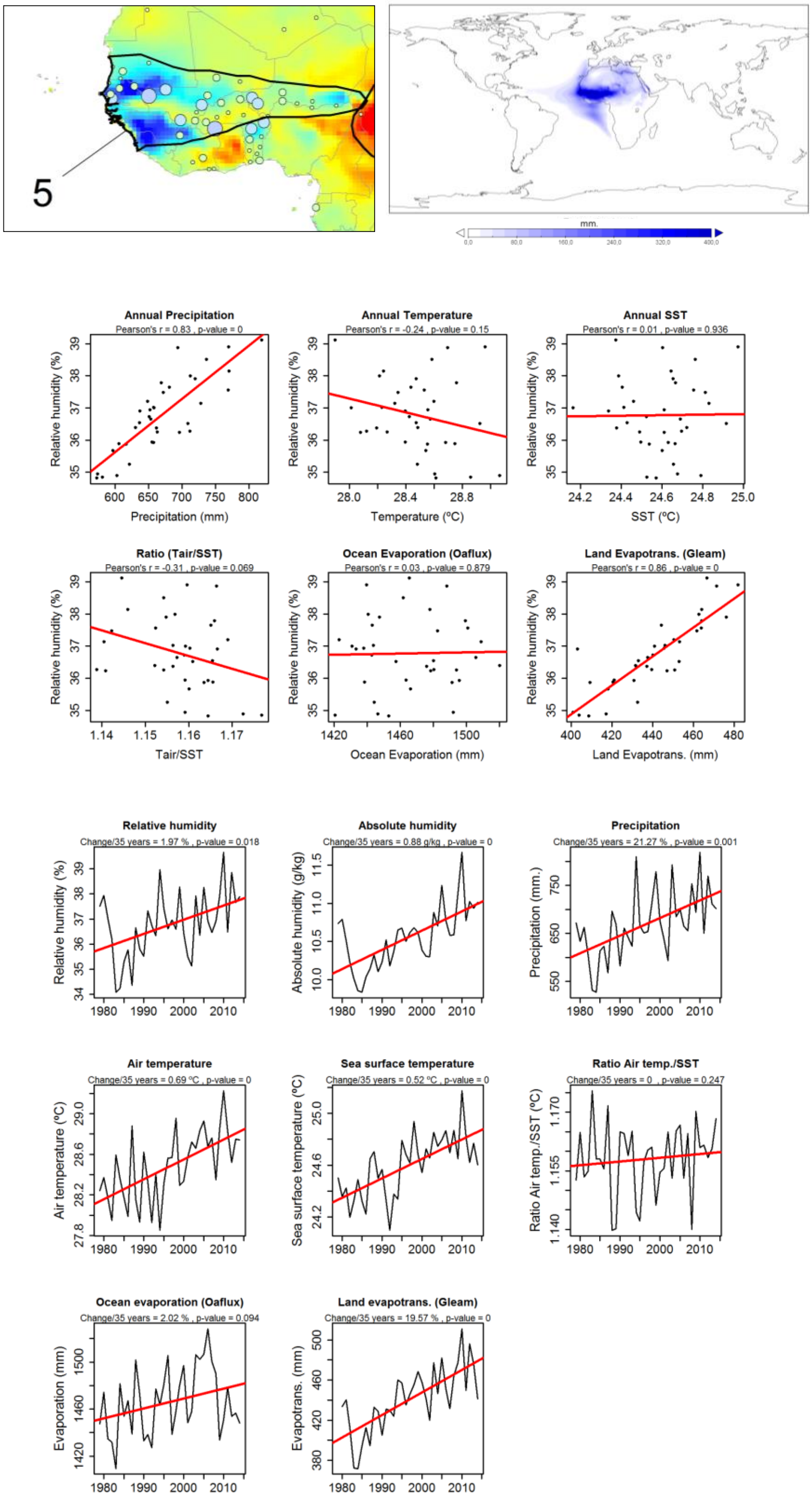

Figure 6: Top left: Annual RH humidity trends in the West Sahel (region 6), Top right: average (E-P)>0 at the annual scale to identify the main humidity sources in the region (mm year^{-1}). Center: Relationship between the de-trended annual RH and the de-trended annual variables for 1979-2014. Bottom: Annual evolution of the different variables corresponding to the West Sahel region. The magnitude of change and significance of the trend is indicated for each variable.

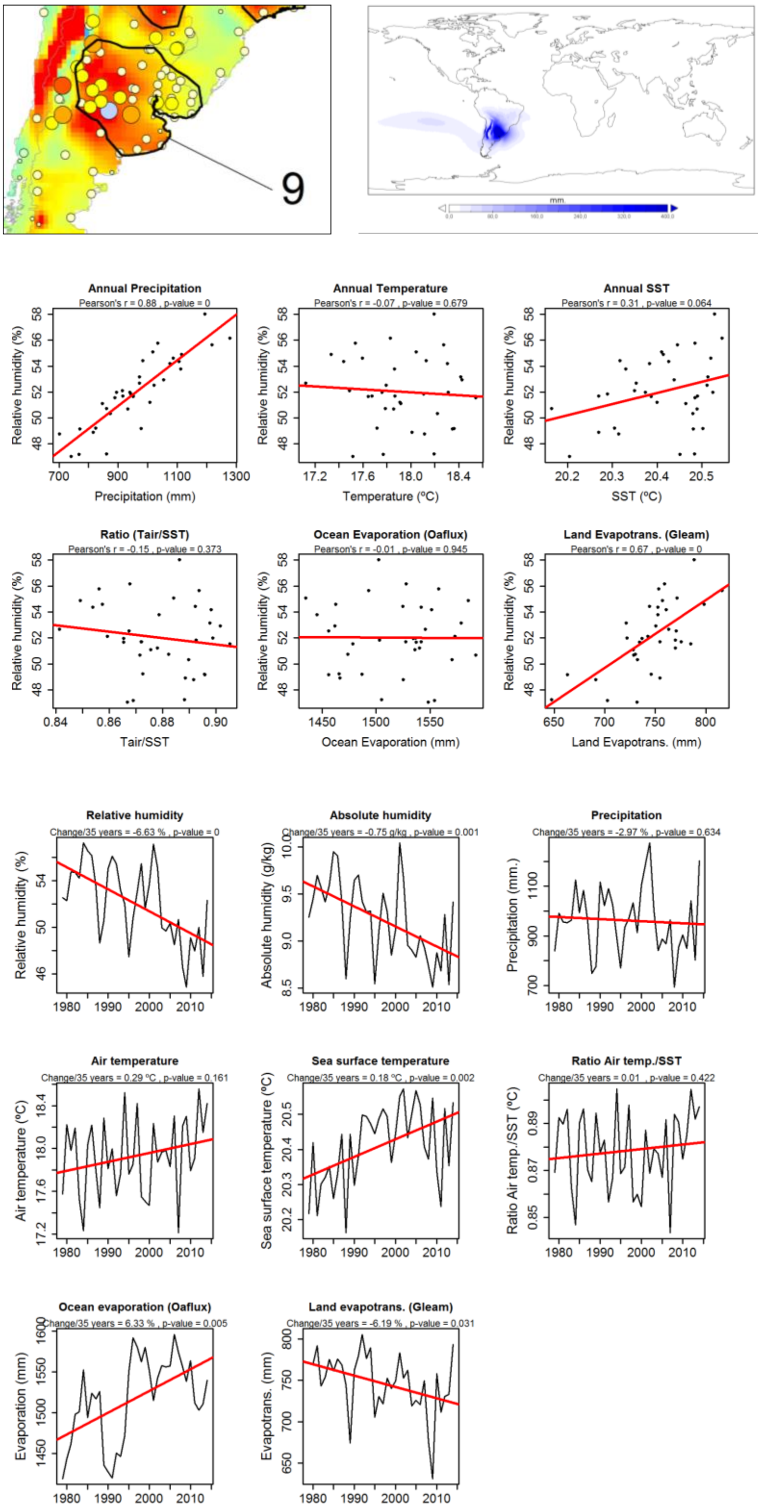

Figure 7: The same as Fig. 6 but for La Plata (region 9).

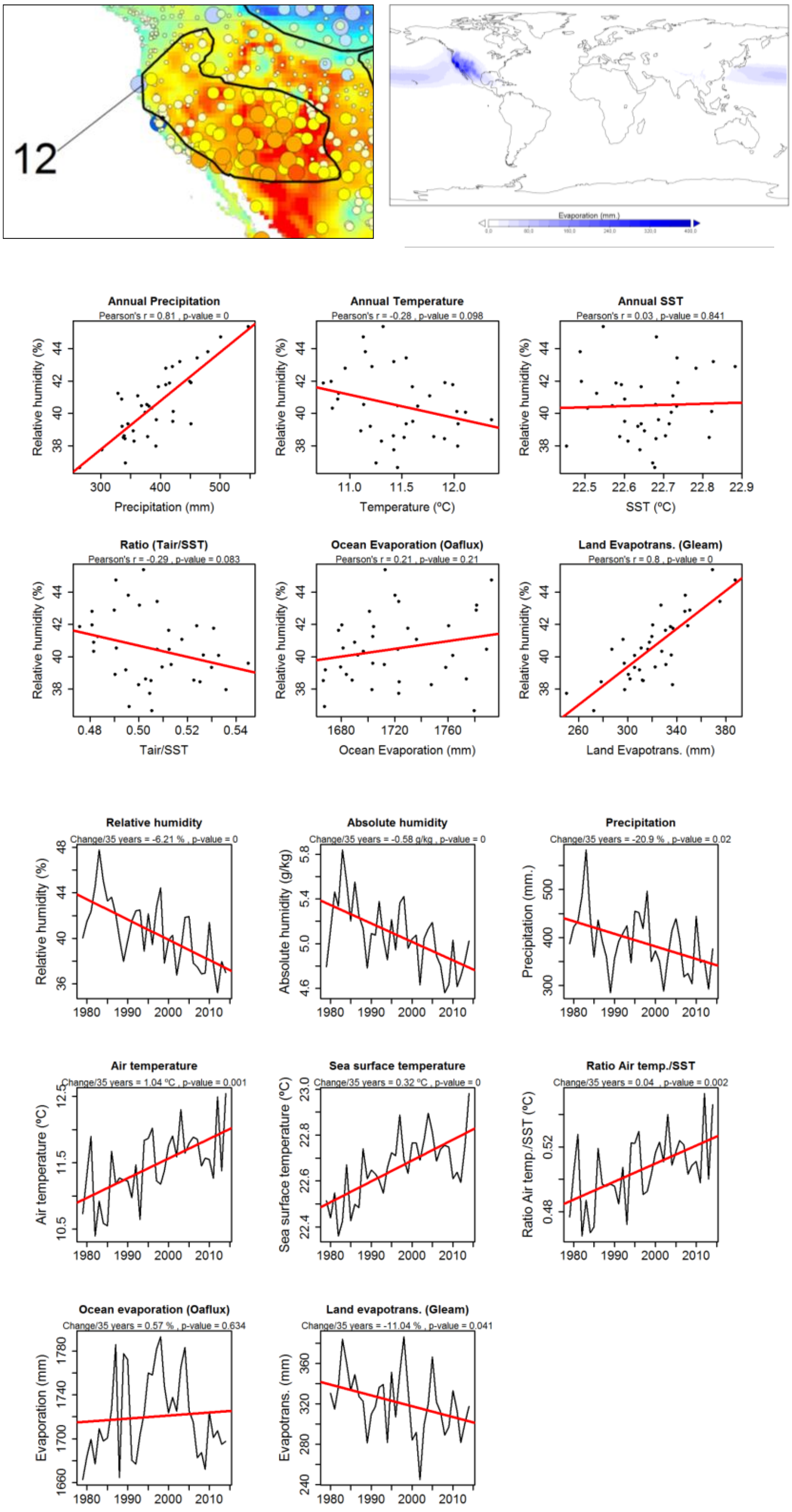

Figure 8: The same as Fig. 6 but for West North America (region 12).

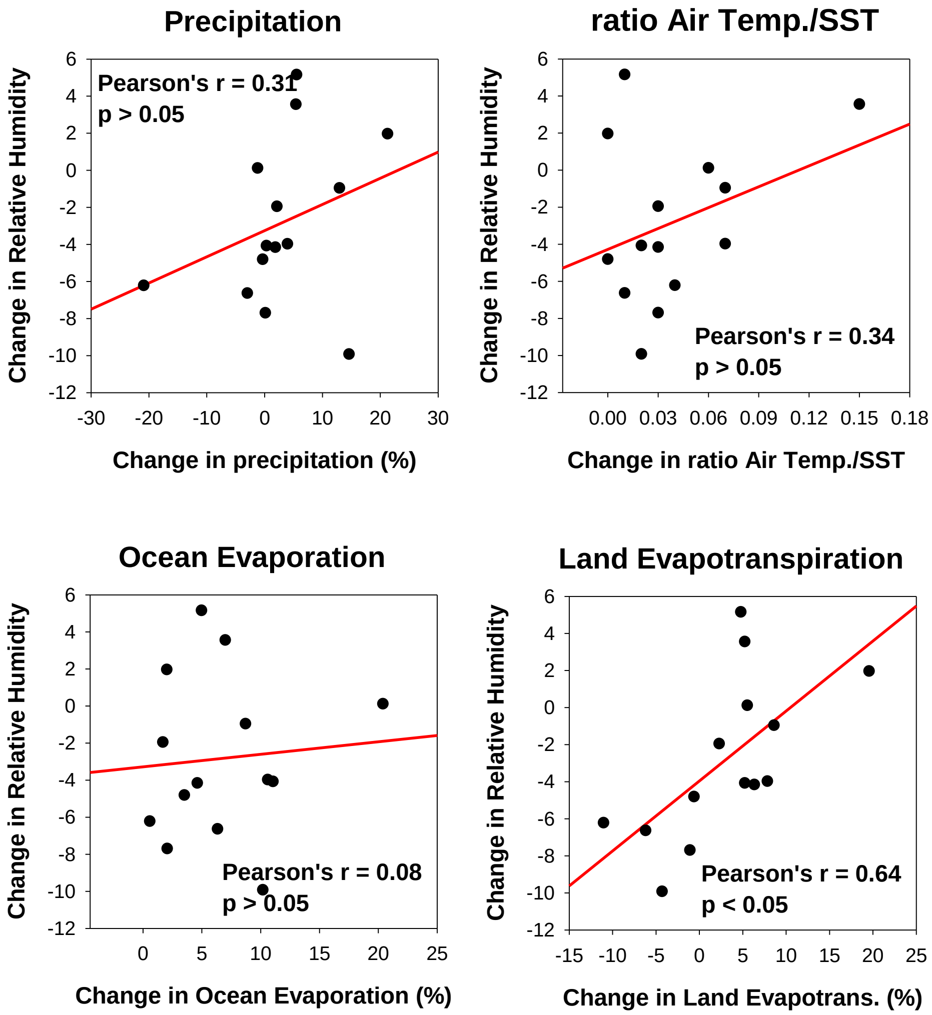

Figure 9: Relationship between the average annual magnitude of change in RH identified in each one of the 14 analyzed regions and the annual magnitude of change in precipitation, the ratio between air temperature/SST, oceanic evaporation and land evapotranspiration.

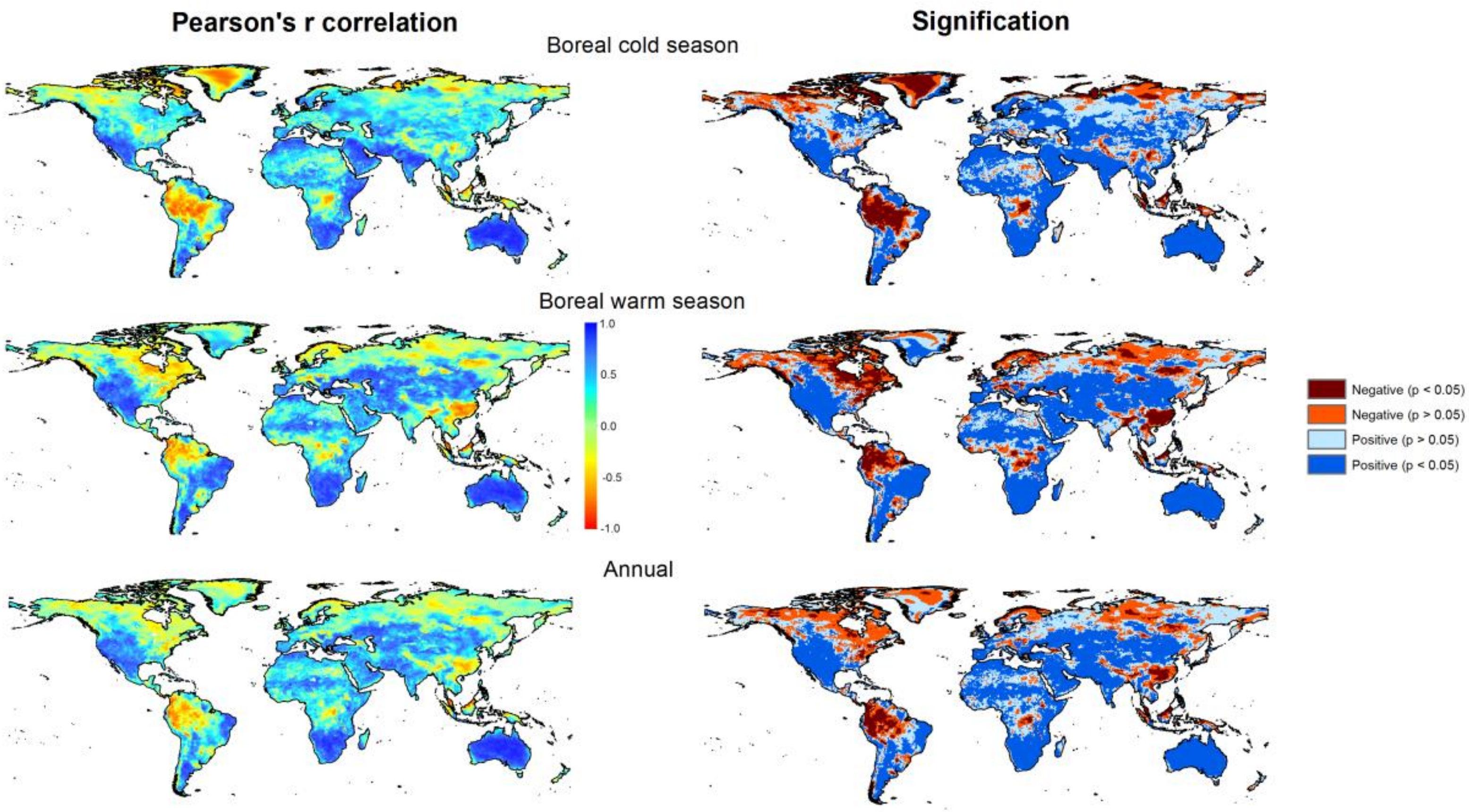

Figure 10: Spatial distribution of the Pearson's r correlations between the detrended RH and land evapotranspiration series at the annual and seasonal time scales. The statistical significance of the correlations is also shown.

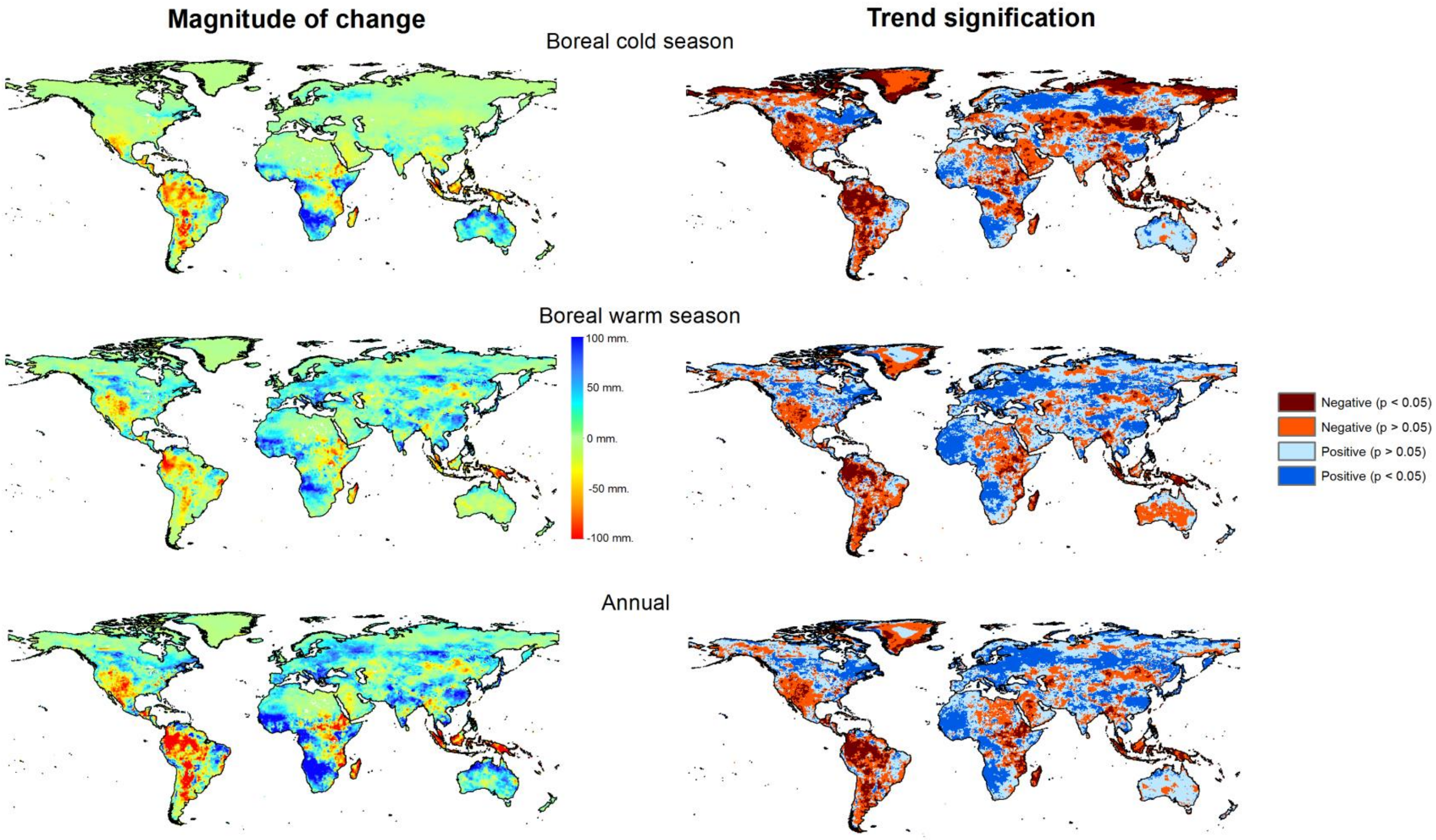

Figure 11: Spatial distribution of the magnitude of change in the annual and seasonal land evapotranspiration (1979-2014) and statistical significance of trends.

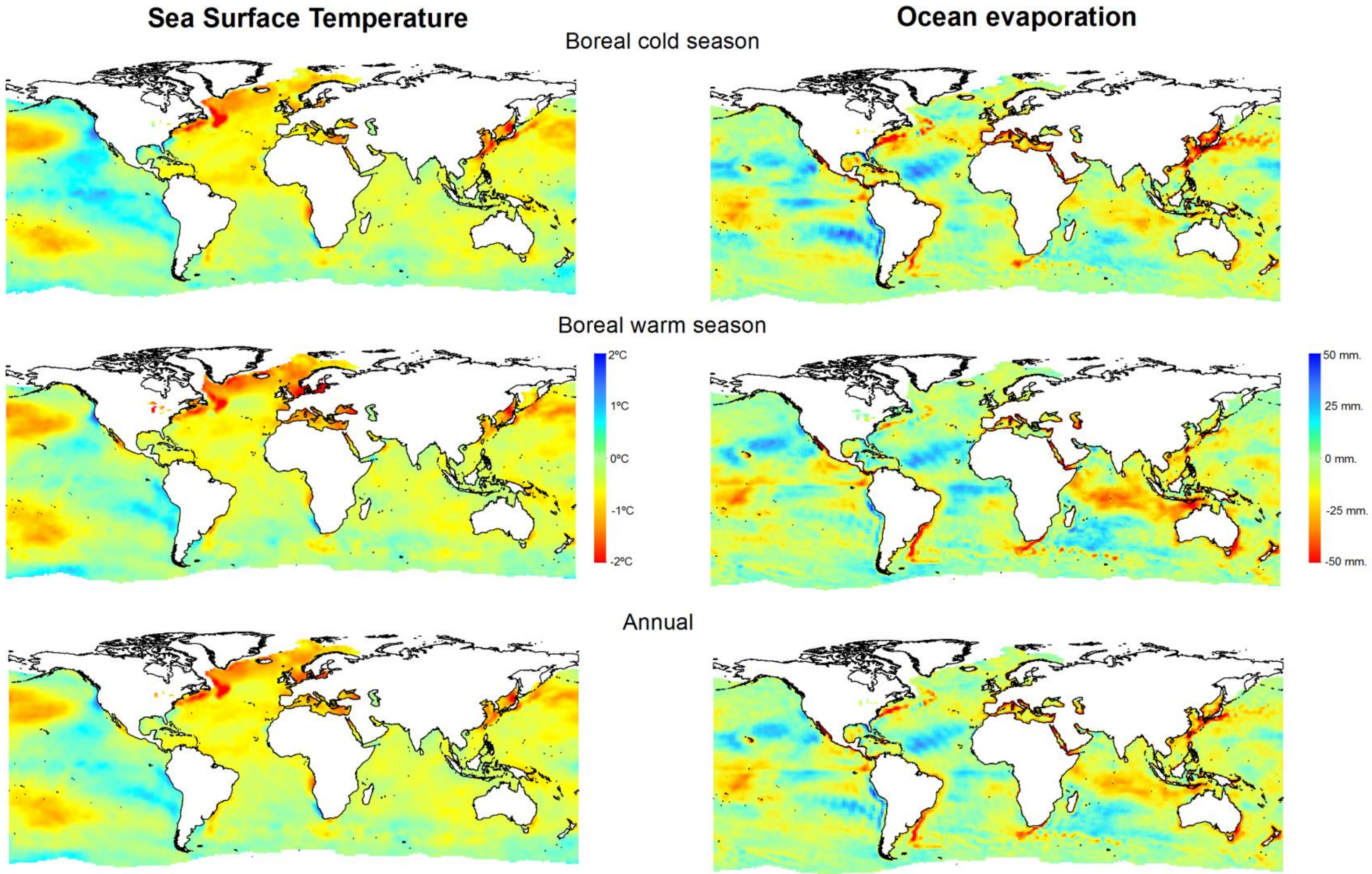

Figure 12: Annual and seasonal magnitude of change of SST and OAFLUX oceanic evaporation for 1979-2014.